

# Gaussian orthogonal latent factor processes for large incomplete matrices of correlated data

Mengyang\* and Hanmo Li†

## Abstract

We introduce the Gaussian orthogonal latent factor processes for modeling and predicting large correlated data. To handle the computational challenge, we first decompose the likelihood function of the Gaussian random field with multi-dimensional input domain into a product of densities at the orthogonal components with lower dimensional inputs. The continuous-time Kalman filter is implemented to efficiently compute the likelihood function without making approximation. We also show that the posterior distribution of the factor processes are independent, as a consequence of prior independence of factor processes and orthogonal factor loading matrix. For studies with a large sample size, we propose a flexible way to model the mean in the model and derive the closed-form marginal posterior distribution. Both simulated and real data applications confirm the outstanding performance of this method.

**Keywords**— Orthogonality, marginalization, correlated data, Gaussian processes

## 1 Introduction

Large spatial, spatio-temporal and functional data are commonly used in various studies to facilitate scientific discoveries, including geohazard quantification, environmental engineering, computer model simulations, and medical imaging. Many data sets are often observed on an incomplete matrix or array with irregular missing values due to the limitation of technique, budget or computational cost.

Gaussian processes (GPs), or Gaussian random fields are widely used for modeling correlated data (Banerjee et al., 2014; Cressie and Cassie, 1993; Rasmussen, 2006). Computing the likelihood function from a GP model generally takes  $O(N_o^3)$  operations in finding the inverse and determinant of the covariance matrix, where  $N_o$  is the number of observations. The computational bottleneck prevents applying a GP model to a large correlated data set directly. Tremendous efforts have been made to approximate the GP model in recent

---

\*Department of Statistics and Applied Probability, University of California, Santa Barbara, CA, Email: mengyang@pstat.ucsb.edu

†Department of Statistics and Applied Probability, University of California, Santa Barbara, CA 93106, USA, Email: hanmo@pstat.ucsb.edu

studies, including, for example, stochastic partial differential equation approach (Lindgren et al., 2011; Rue et al., 2009), hierarchical nearest neighbor methods (Datta et al., 2016), multi-resolution process (Katzfuss, 2017), local Gaussian process approach (Gramacy and Apley, 2015), periodic embedding (Stroud et al., 2017; Guinness and Fuentes, 2017) and covariance tapering (Kaufman et al., 2008). These methods have obtained wide attention in recent years.

In this work, we propose a flexible and computationally feasible approach to model large incomplete matrix observations of correlated data, called the Gaussian orthogonal latent factor (GOLF) processes. We assume the latent processes are defined on two types of disjoint inputs denoted as  $\mathbf{s}$  and  $\mathbf{x}$ . In modeling spatial correlated data, we let  $s$  and  $x$  denote the latitude and longitude, respectively, and in spatio-temporal modeling, the spatial coordinates and time point can be defined as  $\mathbf{s}$  and  $x$ , respectively. Other applications include emulating computationally expensive simulators with solutions on a spatial domain (with the coordinate denoted as  $\mathbf{s}$ ) for a set of parameters and initial conditions  $\mathbf{x}$ . We propose a latent factor model, where each factor is assumed to follow a Gaussian process on input  $\mathbf{x}$ , and the factor loadings are a function of input  $\mathbf{s}$ . After marginalizing out the factor processes, the likelihood of the Gaussian random field with multi-dimensional input domain can be written as a product of densities of orthogonal components with lower dimensional inputs. Furthermore, we show that prior independence between the factor processes results in posterior independence, another important feature for scalable computation. These properties of the GOLF processes are used along with the continuous-time Kalman filter to compute the likelihood and predictive distribution in an computationally efficient way.

A few GP models with a separable covariance function are special cases of the GOLF model. The covariance of the GOLF processes, however, is not separable in general, since the covariance function of each factor process is allowed to be different to model distinct smoothness levels of factor processes. The factor loading matrix of GOLF processes are assumed to be orthogonal and parameterized by input parameter  $\mathbf{s}$ . The orthogonal factor loading matrix allows us to efficiently factorize the likelihood, which results in posterior independence between factor processes that dramatically reduces the computational complexity.

Another related study to this work is the generalized probabilistic principal component analysis (GPPCA) (Gu and Shen, 2020), where the closed-form maximum marginal likelihood estimator of the factor loadings and predictive distributions are derived. We highlight four contributions compared to the GPPCA and other approaches. First and foremost, we consider modeling the incomplete matrix or array with irregular patterns of missing values, whereas the observations are required to be a matrix in the GPPCA. Secondly, we derive the closed-form marginal posterior distribution for identifiability problems, which occurs in sampling from the full conditional distributions. Thirdly, we model the factor loading matrix as a function of the input  $\mathbf{s}$  in this work, whereas the factor loadings are estimated by the maximum marginal likelihood estimator in the GPPCA without the information from the input  $\mathbf{s}$ . Besides, as the large number of observations provides rich information to identify the local trend, we introduce a flexible way to model the mean function, and derive the marginal posterior distribution of the linear coefficients after integrating out the factor processes. Despite the difference between these two models, the GPPCA and Bayesian inference of GOLF processes proposed in this work are both guided by deriving the closed-form expressions of the marginal densities after integrating out the factor processes for predictions

and uncertainty quantification.

GOLF processes are computationally feasible for large data due to orthogonal decomposition of the likelihood and posterior independence of the factor processes. We are able to obtain full Bayesian inference for large spatial, spatio-temporal and functional data. For spatially correlated data on an incomplete lattice, computing the likelihood of the GOLF model has computational complexity  $O(Nd)$ , where  $d$  is the number of factors and  $N = n_1 n_2$  with  $n_1$  and  $n_2$  being the number of coordinates in latitude and longitude, respectively. For spatio-temporal data, the computational complexity is  $O(N \max(d_1, d_2))$  with  $d_1$  and  $d_2$  being the factors for latitude and longitude, and  $d = d_1 d_2$  being the total number of factors. See Section 3.3 for detailed discussion of the computational complexity of the GOLF model in different scenarios.

Both simulated and real data analysis confirm the excellent performance in prediction by the GOLF model. In the first real dataset, for instance, we compare our method with the other methods on predicting the irregular missing values of temperature datasets at the  $300 \times 500$  lattice in Heaton et al. (2019). In the second real application, we apply our model to interpolate the monthly spatio-temporal temperature anomalies of the earth from U.S. National Oceanic and Atmospheric Administration (NOAA). Unlike Gu and Shen (2020) where the missing data are assumed to be a matrix at the same locations over particular months, here we hold out test data at randomly sampled test locations and time points, which is closer to the real scenario.

The rest of the article is organized as follows. In Section 2.1, we introduce the GOLF model with an emphasis on orthogonal decomposition of the likelihood function and posterior independence of latent factor processes. The flexible mean function, spatial latent factor loading matrix and kernel functions are discussed in Section 2.2-2.4, respectively. We introduce the Markov Chain Monte Carlo (MCMC) algorithm and discuss the computational complexity in Section 3.1. In Section 3.2, we apply the continuous-time Kalman filter in computing the likelihood of the projected outcomes with linear computational complexity without approximation. We compare our model with the alternatives using various simulated examples and real examples in Section 5 and Section 6, respectively. We conclude this work and discuss several potential extensions in Section 7.

## 2 Gaussian orthogonal latent factor processes

### 2.1 Orthogonal decomposition and posterior independence

Let  $\mathbf{y}_s(\mathbf{x}) = (y_{s_1}(\mathbf{x}), \dots, y_{s_{n_1}}(\mathbf{x}))^T$  be an  $n_1 \times 1$  vector of observations at coordinates  $\mathbf{s} =: (\mathbf{s}_1, \dots, \mathbf{s}_{n_1})^T$  with  $\mathbf{s}_i \in \mathbb{R}^{p_1}$  for  $i = 1, \dots, n_1$  and input  $\mathbf{x} \in \mathbb{R}^{p_2}$ . Consider the latent factor model:

$$\mathbf{y}_s(\mathbf{x}) = \mathbf{m}_s(\mathbf{x}) + \mathbf{A}_s \mathbf{z}(\mathbf{x}) + \boldsymbol{\epsilon}, \quad (1)$$

where  $\boldsymbol{\epsilon} \sim \mathcal{N}(0, \sigma_0^2 \mathbf{I}_{n_1})$  being a vector of independent Gaussian noise,  $\mathbf{A}_s = [\mathbf{a}_1, \dots, \mathbf{a}_d]$  is a  $n_1 \times d$  factor loading matrix and  $\mathbf{z}(\mathbf{x}) = (z_1(\mathbf{x}), \dots, z_d(\mathbf{x}))^T$  is a  $d$ -dimensional factor processes with  $d \leq n_1$ . The mean function  $\mathbf{m}_s(\mathbf{x}) = (m_{s_1}(\mathbf{x}), \dots, m_{s_{n_1}}(\mathbf{x}))^T$  is typically modeled via a linear trend of regressors, which will be discussed in Section 2.2.

As the data are typically positively correlated at two nearby inputs, we assume  $z_l(\cdot)$  independently follows a zero-mean Gaussian process (GP), meaning that for any  $\{\mathbf{x}_1, \dots, \mathbf{x}_{n_2}\}$ ,  $\mathbf{Z}_l^T = (Z_l(\mathbf{x}_1), \dots, Z_l(\mathbf{x}_{n_2}))^T$  is a multivariate normal distribution

$$(\mathbf{Z}_l^T \mid \Sigma_l) \sim \mathcal{N}(\mathbf{0}, \Sigma_l) \quad (2)$$

where the  $(i, j)$ th entry of the covariance matrix is  $\sigma_l^2 K_l(\mathbf{x}_i, \mathbf{x}_j)$  with kernel function  $K_l(\cdot, \cdot)$  and variance parameter  $\sigma_l^2$ , for  $l = 1, \dots, d$ . Here we assume independence between the factor processes *a priori*. We will soon show that the prior independence implies the posterior independence when the factor loading matrix is orthogonal. Model (1) can be viewed as a special case of the linear model of coregionalization (Gelfand et al., 2004) widely used in applied in modeling multivariate spatially correlated data and functional data. A detailed comparison between our approach and other related approaches is discussed in Section 4.

Note that only the  $d$ -dimensional linear subspace of factor loadings  $\mathbf{A}_s$  can be identified if not further specification of factor loading matrix  $\mathbf{A}_s$  is made, as the model (1) is unchanged if the pair  $(\mathbf{A}_s, \mathbf{z}(\mathbf{x}))$  is replaced by  $(\mathbf{A}_s \mathbf{G}, \mathbf{G}^{-1} \mathbf{z}(\mathbf{x}))$  for any invertible matrix  $\mathbf{G}$ . Besides, computation could be challenging when the number of factors or input parameters is large. Thus, we assume that the column of  $\mathbf{A}_s$  is orthonormal.

**Assumption 1.**

$$\mathbf{A}_s^T \mathbf{A}_s = \mathbf{I}_d. \quad (3)$$

Assumption (3) may be replaced by  $\mathbf{A}_s^T \mathbf{A}_s = \mathbf{\Lambda}$ , where  $\mathbf{\Lambda}$  is a diagonal matrix. Since we estimate variance parameters  $\boldsymbol{\sigma}^2 = (\sigma_1^2, \dots, \sigma_d^2)^T$  of latent factor processes by data, diagonal terms of  $\mathbf{\Lambda}$  are redundant. Thus we proceed with the Assumption 1 herein.

Let us first assume we have an  $n_1 \times n_2$  matrix of observations  $\mathbf{Y} = [\mathbf{y}_s(\mathbf{x}_1), \dots, \mathbf{y}_s(\mathbf{x}_{n_2})]$  at inputs  $\{\mathbf{x}_1, \dots, \mathbf{x}_{n_2}\}$ , and then we extend our method to incomplete matrix observations in the Section 3. Denote  $\mathbf{B}$  the regression parameters in the  $n_1 \times n_2$  mean matrix  $\mathbf{M} = (\mathbf{m}_s(\mathbf{x}_1), \dots, \mathbf{m}_s(\mathbf{x}_{n_2}))$ . Denote  $\boldsymbol{\Theta} = (\mathbf{A}_s, \mathbf{B}, \boldsymbol{\sigma}^2, \boldsymbol{\gamma})$ , which contains the factor loadings, mean parameters, variance parameters and range parameters in the kernel functions. Further let  $\mathbf{A}_F = [\mathbf{A}_s, \mathbf{A}_c] = [\mathbf{a}_1, \mathbf{a}_2, \dots, \mathbf{a}_{n_1}]$ , where  $\mathbf{A}_c$  is an  $n_1 \times (n_1 - d)$  matrix of the orthogonal complement of  $\mathbf{A}_s$ . Assumption 1 allows us to decompose the marginal likelihood (after integrating out the random factor  $\mathbf{Z}$ ) into a product of multivariate normal densities of the outcomes at the projected coordinates:

$$p(\mathbf{Y} \mid \boldsymbol{\Theta}) = \prod_{l=1}^d \mathcal{PN}(\tilde{\mathbf{y}}_l; \mathbf{0}, \tilde{\Sigma}_l) \prod_{l=d+1}^{n_1} \mathcal{PN}(\tilde{\mathbf{y}}_l; \mathbf{0}, \sigma_0^2 \mathbf{I}_{n_1}), \quad (4)$$

where  $\tilde{\mathbf{y}}_l = (\mathbf{Y} - \mathbf{M})^T \mathbf{a}_l$  for  $l = 1, \dots, d$ , and  $\tilde{\mathbf{y}}_l = (\mathbf{Y} - \mathbf{M})^T \mathbf{a}_l$  with  $\mathbf{a}_l$  being the  $(l - d)$ th column of  $\mathbf{A}_c$  for  $l = d + 1, \dots, n_1$ ,  $\tilde{\Sigma}_l = \Sigma_l + \sigma_0^2 \mathbf{I}_{n_2}$  and  $\mathcal{PN}(\cdot; \boldsymbol{\mu}, \Sigma)$  denotes the density of the multivariate normal distribution with mean  $\boldsymbol{\mu}$  and covariance matrix  $\Sigma$ . In practice, note that we can avoid computing  $\mathbf{A}_c$  by using the identity  $\mathbf{A}_s \mathbf{A}_s^T + \mathbf{A}_c \mathbf{A}_c^T = \mathbf{I}_{n_1}$ . Equation (4) is a consequence of Lemma 1 in (Gu and Shen, 2020) and the derivation is given in the supplementary materials.

The orthogonal factor loading matrix in Assumption 1 and prior independence of factor processes lead to the posterior independence of the factor processes, introduced in the following corollary.

**Corollary 1.** *For model (1) with Assumption 1:*

1. *The covariance of the posterior marginal distributions of any two factor processes is zero:  $\text{Cov}[\mathbf{Z}_l^T, \mathbf{Z}_m^T \mid \mathbf{Y}, \boldsymbol{\Theta}] = \mathbf{0}_{n_2 \times n_2}$ , where  $l = 1, \dots, d$ ,  $m = 1, \dots, d$  and  $l \neq m$ .*
2. *For  $l = 1, \dots, d$ , the posterior distribution  $(\mathbf{Z}_l^T \mid \mathbf{Y}, \boldsymbol{\Theta})$  follows a multivariate normal distribution*

$$\mathbf{Z}_l^T \mid \mathbf{Y}, \boldsymbol{\Theta} \sim \mathcal{N}(\boldsymbol{\mu}_{Z_l}, \boldsymbol{\Sigma}_{Z_l}), \quad (5)$$

*where  $\boldsymbol{\mu}_{Z_l} = \boldsymbol{\Sigma}_l \tilde{\boldsymbol{\Sigma}}_l^{-1} \tilde{\mathbf{y}}_l$  and  $\boldsymbol{\Sigma}_{Z_l} = \boldsymbol{\Sigma}_l - \boldsymbol{\Sigma}_l \tilde{\boldsymbol{\Sigma}}_l^{-1} \boldsymbol{\Sigma}_l$  with  $\tilde{\boldsymbol{\Sigma}}_l = \boldsymbol{\Sigma}_l + \sigma_0^2 \mathbf{I}_{n_2}$ , for  $l = 1, \dots, d$ .*

The proof of Corollary 1 is given in the supplementary materials. We call the latent factor processes in (1) with Assumption 1 *Gaussian orthogonal latent factor* (GOLF) processes, because of orthogonal decomposition of the likelihood function and posterior independence between two factor processes. These two properties dramatically ease the computational burden, as we will see in Section 3.

The posterior distribution of  $\mathbf{Z}_l$  for  $l = 1, \dots, d$  has a clear interpretation. We first project the centered observational matrix onto the new coordinate system through  $\tilde{\mathbf{Y}} := \mathbf{A}^T(\mathbf{Y} - \mathbf{M})$ . The  $l$ th row of  $\tilde{\mathbf{Y}}$  is the observations at the  $l$ th orthogonal coordinate. The posterior distribution of  $\mathbf{Z}$  is a product of the marginal posterior distribution of  $\mathbf{Z}_l^T$  due to independence between the projected outcomes, and  $p(\mathbf{Z}_l^T \mid \mathbf{Y}, \boldsymbol{\Theta})$  is the posterior of the mean of the projected observations at the  $l$ th orthogonal coordinate for  $l = 1, \dots, d$ . The main idea here is to decompose the likelihood of GP models with multi-dimensional inputs by a product of densities with low dimension input, and to utilize the continuous time Kalman Filter for fast computation introduced in Section 3.2.

Other than the spatial and spatio-temporal data sets, model (1) is also widely used for emulating computationally expensive computer models with multivariate output variables (Higdon et al., 2008; Paulo et al., 2012). When the observations can be written as a matrix, the computational benefits from Assumption 1 are exploited in Gu and Shen (2020). However, various data sets, such as climate datasets and satellite radar interferograms (Heaton et al., 2019; Anderson et al., 2019), have irregularly missing values (i.e. the observations are not a matrix). In this work, we introduce a computationally efficient model for incomplete matrix or array observations with irregular missing values. Before moving on to the topics of computational strategy, we first introduce a flexible way to model the mean functions for large data.

## 2.2 Flexible mean function and marginalization

The mean function  $m_s(\cdot)$  plays an important role in modeling and predicting correlated data. The mathematical models or computer models (such as numerical solution of partial differential equations), for example, can be included as a part of the mean in computer model calibration and prediction (Kennedy and O'Hagan, 2001). Regressors, other than  $\mathbf{s}$  or  $\mathbf{x}$ ,

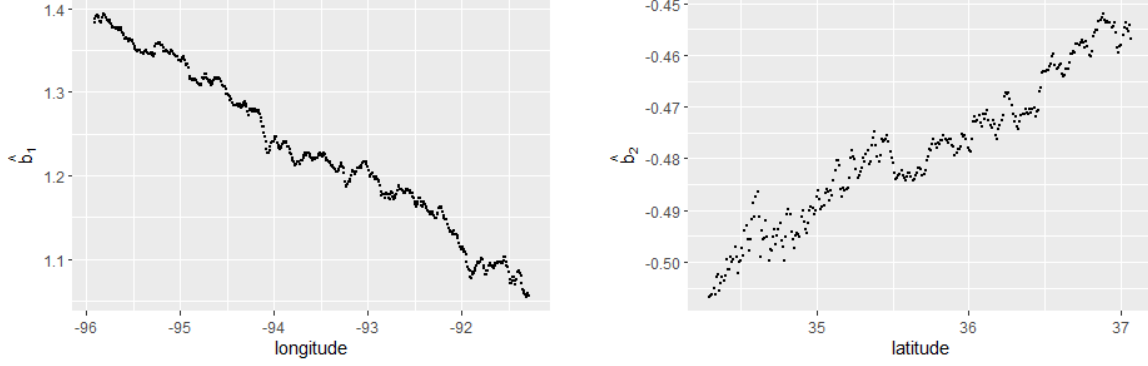


Figure 1: Estimated linear coefficients for temperature observations in Heaton et al. (2019). In the left panel, the dots are the estimated coefficients in a linear regression of observations at each longitude separately using latitudes as regressors. The estimated linear coefficients for the observations at each latitude are graphed in the right panel, where longitudes are used as regressors.

may also be included in the mean function to improve the predictive accuracy. Here for simplicity we assume we only use a basis function of  $\mathbf{s}$  and  $\mathbf{x}$  to model the mean. Additional terms may be included in the mean if available.

The mean function often consists of a linear model of regressors, where the regression coefficients are shared by column observations or row observations. For instance, the mean function may be modeled as  $\mathbf{m}_s(\mathbf{x}) = \mathbf{h}_1(\mathbf{s})\mathbf{b}_{1,0}$ , or  $\mathbf{m}_s(\mathbf{x}) = \mathbf{h}_2(\mathbf{x})\mathbf{b}_{2,0}$ , where  $\mathbf{h}_1(\mathbf{s})$  and  $\mathbf{h}_2(\mathbf{x})$  are a set of  $1 \times q_1$  and  $1 \times q_2$  mean basis functions with  $\mathbf{b}_{1,0}$  and  $\mathbf{b}_{2,0}$  being  $q_1 \times 1$  and  $q_2 \times 1$  regression coefficients, respectively. The regression coefficients  $\mathbf{b}_{1,0}$ , for example, are shared across each  $\mathbf{x}$ .

The shared regression coefficients may be a restrictive assumption when data sets are large. Consider, for instance, the temperature data set used in Heaton et al. (2019), where the temperature values are shown in Figure 5. In Figure 1, we graph the fitted linear regression coefficients using latitudes or longitudes as regressors. The estimated regression coefficients are not the same across latitude or longitude. In practice, one may include the intercept and spatial random effect in the analysis. A detailed comparison of different approaches on this data set is given in Section 6.1.

A natural extension of modeling the mean function is to allow the mean parameters at each row or column of the observations to be different, e.g.  $\mathbf{m}_{s_i}(\mathbf{x}_j) = \mathbf{h}_1(\mathbf{s}_i)\mathbf{b}_{1,j}$ , or  $\mathbf{m}_{s_i}(\mathbf{x}) = \mathbf{h}_2(\mathbf{x})\mathbf{b}_{2,i}$ , for  $i = 1, \dots, n_1$  and  $j = 1, \dots, n_2$ . Some choices of the individual mean functions are summarized in Table 1. The shared mean functions are special cases of individual mean functions, when  $\mathbf{b}_{1,j} = \mathbf{b}_{1,k}$  and  $\mathbf{b}_{2,m} = \mathbf{b}_{2,l}$  for any  $1 \leq j, k \leq n_2$  and  $1 \leq l, m \leq n_1$ . Compared to models with shared coefficient parameters, models with different regression coefficients are more flexible to capture the trend when observations are large. The mean function may be specified based on model interpretation, or based on exploratory data analysis.

To implement full Bayesian inference of the parameters, one may sample from the posterior distribution of regression parameters  $p(\mathbf{B} \mid \boldsymbol{\Theta}_{-B}, \mathbf{Y}, \mathbf{Z})$ . However, we found a severe identifiability problem between the mean  $\mathbf{M}$  and  $\mathbf{AZ}$ , when the regression coefficients  $\mathbf{B}$

Individual mean	$\mathbf{m}_{s_i}(\mathbf{x}_j)$	$\mathbf{M}$	coefficients $\mathbf{B}$
Linear trend of $\mathbf{s}$	$\mathbf{h}_1(\mathbf{s}_i)\mathbf{b}_{1,j}$	$\mathbf{H}_1\mathbf{B}_1$	$\mathbf{B}_1$
Linear trend of $\mathbf{x}$	$\mathbf{h}_2(\mathbf{x}_j)\mathbf{b}_{2,i}$	$(\mathbf{H}_2\mathbf{B}_2)^T$	$\mathbf{B}_2$
Mixed linear trend	$\mathbf{h}_1(\mathbf{s}_i)\mathbf{b}_{1,j} + \mathbf{h}_2(\mathbf{x}_j)\mathbf{b}_{2,i}$	$\mathbf{H}_1\mathbf{B}_1 + (\mathbf{H}_2\mathbf{B}_2)^T$	$[\mathbf{B}_1, \mathbf{B}_2]$

Table 1: Summary of the mean function studied in this work. In the third column,  $\mathbf{H}_1 = (\mathbf{h}_1^T(\mathbf{s}_1), \dots, \mathbf{h}_1^T(\mathbf{s}_{n_1}))^T$  and  $\mathbf{H}_2 = (\mathbf{h}_2^T(\mathbf{x}_1), \dots, \mathbf{h}_2^T(\mathbf{x}_{n_2}))^T$  are  $n_1 \times q_1$  and  $n_2 \times q_2$  mean basis matrices, respectively. Regression coefficients are denoted as  $\mathbf{B}_1 = (\mathbf{b}_{1,1}, \dots, \mathbf{b}_{1,n_2})$  and  $\mathbf{B}_2 = (\mathbf{b}_{2,1}, \dots, \mathbf{b}_{2,n_1})$  for the basis function  $\mathbf{h}_1(\cdot)$  and  $\mathbf{h}_2(\cdot)$ , respectively.

are sampled from the full posterior distribution. This is because the likelihood function of the mean parameters is flat when data are very correlated. Consequently, the absolute values of the entries of these two matrices can be very big, making the MCMC algorithm very unstable. To alleviate the identifiability problem, we first marginalize out factors  $\mathbf{Z}$  and sample regression parameters from the marginal posterior distribution  $p(\mathbf{B} \mid \boldsymbol{\Theta}_{-B}, \mathbf{Y})$ . The marginal posterior distributions of the regression parameters are given in the following Theorem 1 and Theorem 2. The proofs are given in supplementary materials.

**Theorem 1.** 1. (Row regression coefficients). Assume  $\mathbf{M} = \mathbf{H}_1\mathbf{B}_1$  and the objective prior  $\pi(\mathbf{B}_1) \propto 1$  for  $\mathbf{B}_1$ . After marginalizing out the factor  $\mathbf{Z}$ , the posterior samples of  $\mathbf{B}_1$  from  $p(\mathbf{B}_1 \mid \mathbf{Y}, \boldsymbol{\Theta}_{-B_1})$  can be obtained by

$$\mathbf{B}_1 = \hat{\mathbf{B}}_1 + (\mathbf{H}_1^T \mathbf{H}_1)^{-1} \mathbf{H}_1^T \mathbf{A}_s \tilde{\mathbf{B}}_{1,0,s}^T + \sigma_0 (\mathbf{H}_1^T \mathbf{H}_1)^{-1} \mathbf{H}_1^T (\mathbf{I}_{n_1} - \mathbf{A}_s \mathbf{A}_s^T) \mathbf{Z}_{0,1} \quad (6)$$

where  $\hat{\mathbf{B}}_1 = (\mathbf{H}_1^T \mathbf{H}_1)^{-1} \mathbf{H}_1^T \mathbf{Y}$ ,  $\tilde{\mathbf{B}}_{1,0,s}$  is an  $n_2 \times d$  matrix with the  $l$ th column independently sampled from  $\mathcal{N}(\mathbf{0}, \tilde{\boldsymbol{\Sigma}}_l)$  for  $l = 1, \dots, d$ , and  $\mathbf{Z}_{0,1}$  is an  $n_1 \times n_2$  matrix with each entry independently sampled from the standard normal distribution.

2. (Column regression coefficients). Assume  $\mathbf{M} = (\mathbf{H}_2\mathbf{B}_2)^T$  and the objective prior  $\pi(\mathbf{B}_2) \propto 1$  for the regression parameters  $\mathbf{B}_2$ . After marginalizing out the factor  $\mathbf{Z}$ , the posterior samples of  $\mathbf{B}_2$  from  $p(\mathbf{B}_2 \mid \mathbf{Y}, \boldsymbol{\Theta}_{-B_2})$  can be obtained by

$$\mathbf{B}_2 = \hat{\mathbf{B}}_2 + \tilde{\mathbf{B}}_{2,0,s} \mathbf{A}_s^T + \sigma_0 \mathbf{L}_{H_2} \mathbf{Z}_{0,2} (\mathbf{I}_{n_1} - \mathbf{A}_s \mathbf{A}_s^T), \quad (7)$$

where  $\hat{\mathbf{B}}_2 = \sum_{l=1}^d (\mathbf{H}_2^T \tilde{\boldsymbol{\Sigma}}_l^{-1} \mathbf{H}_2)^{-1} \mathbf{H}_2^T \tilde{\boldsymbol{\Sigma}}_l^{-1} \mathbf{Y}^T \mathbf{a}_l \mathbf{a}_l^T + (\mathbf{H}_2^T \mathbf{H}_2)^{-1} \mathbf{H}_2^T \mathbf{Y}^T (\mathbf{I}_{n_1} - \mathbf{A}_s \mathbf{A}_s^T)$  and  $\tilde{\mathbf{B}}_{2,0,s}$  is a  $q_2 \times d$  matrix with the  $l$ th column independently sampled from  $\mathcal{N}(\mathbf{0}, (\mathbf{H}_2^T \tilde{\boldsymbol{\Sigma}}_l^{-1} \mathbf{H}_2)^{-1})$  for  $l = 1, \dots, d$ .  $\mathbf{L}_{H_2}$  is a  $q_2 \times q_2$  matrix such that  $\mathbf{L}_{H_2} \mathbf{L}_{H_2}^T = (\mathbf{H}_2^T \mathbf{H}_2)^{-1}$  and  $\mathbf{Z}_{0,2}$  is a  $q_2 \times n_1$  matrix with each entry independently sampled from the standard normal distribution.

When both the row regression coefficients and column regression coefficients are in the model, we found that  $\mathbf{M}_1 = \mathbf{H}_1\mathbf{B}_1$  and  $\mathbf{M}_2 = (\mathbf{H}_2\mathbf{B}_2)^T$  are not identifiable, if we sample  $\mathbf{B}_1$  and  $\mathbf{B}_2$  from the full conditional distribution. To avoid this problem, we first marginalizing out  $\mathbf{B}_2$  and  $\mathbf{Z}$  to sample  $\mathbf{B}_1$ . Then we condition  $\mathbf{B}_1$  to sample  $\mathbf{B}_2$ . We summarize this approach in the Theorem 2 below.

**Theorem 2.** Assume  $\mathbf{M} = \mathbf{H}_1\mathbf{B}_1 + (\mathbf{H}_2\mathbf{B}_2)^T$  and let the objective prior  $\pi(\mathbf{B}_1, \mathbf{B}_2) \propto 1$  for the regression parameters  $\mathbf{B}_1$  and  $\mathbf{B}_2$ .

1. After marginalizing out  $\mathbf{Z}$  and  $\mathbf{B}_2$ , the marginal posterior sample of  $\mathbf{B}_1$  from  $p(\mathbf{B}_1 \mid \mathbf{Y}, \boldsymbol{\Theta}_{-\mathbf{B}_1, -\mathbf{B}_2})$  can be obtained by

$$\mathbf{B}_1 = \hat{\mathbf{B}}_1 + (\mathbf{H}_1^T \mathbf{H}_1)^{-1} \mathbf{H}_1^T \mathbf{A}_s \tilde{\mathbf{B}}_{1,Q}^T + \sigma_0 (\mathbf{H}_1^T \mathbf{H}_1)^{-1} \mathbf{H}_1^T (\mathbf{I}_{n_1} - \mathbf{A}_s \mathbf{A}_s^T) \mathbf{Z}_{0,1} \mathbf{P}_0, \quad (8)$$

where  $\hat{\mathbf{B}}_1 = (\mathbf{H}_1^T \mathbf{H}_1)^{-1} \mathbf{H}_1^T \mathbf{Y}$ ,  $\tilde{\mathbf{B}}_{1,Q}$  is an  $n_2 \times d$  matrix with the  $l$ th column independently sampled from  $\mathcal{N}(\mathbf{0}, \mathbf{Q}_{1,l})$ , with  $\mathbf{Q}_{1,l} = \mathbf{P}_l \tilde{\boldsymbol{\Sigma}}_l^{-1} \mathbf{P}_l$  where  $\mathbf{P}_l = \mathbf{I}_{n_2} - \mathbf{H}_2 (\mathbf{H}_2^T \tilde{\boldsymbol{\Sigma}}_l^{-1} \mathbf{H}_2)^{-1} \mathbf{H}_2^T \tilde{\boldsymbol{\Sigma}}_l^{-1}$  for  $l = 1, \dots, d$ .  $\mathbf{Z}_{0,1}$  is an  $n_1 \times n_2$  matrix with each entry independently sampled from standard normal distribution and  $\mathbf{P}_0 = (\mathbf{I}_{n_2} - \mathbf{H}_2 (\mathbf{H}_2^T \mathbf{H}_2)^{-1} \mathbf{H}_2^T)$ .

2. The posterior sample of  $\mathbf{B}_2$  from  $p(\mathbf{B}_2 \mid \mathbf{Y}_{B_1}, \boldsymbol{\Theta}_{-\mathbf{B}_2})$  can be obtained through equation (7) by replacing  $\mathbf{Y}$  by  $\mathbf{Y} - \mathbf{H}_1 \mathbf{B}_1$ .

In Theorem 1 and Theorem 2, the marginal posterior distribution of the regression coefficients depends on the  $n_1 \times d$  factor loading matrix, but not the complement of the factor loading matrix ( $\mathbf{A}_c$ ). Thus we do not need to compute  $\mathbf{A}_c$ . The most computationally intensive terms are those containing the covariance matrix  $\boldsymbol{\Sigma}_l$  and its inverse. Fortunately, under certain scenarios, these terms can be computed with linear complexity  $O(n_2)$  without approximation. We discuss this method in Section 3.2.

### 2.3 Spatial latent factor loading matrix

In this section, we discuss a model of the latent factor loading matrix  $\mathbf{A}_s$  that satisfies the orthogonal constraint in (3). As output values are marginally correlated at two inputs  $\mathbf{s}_a$  and  $\mathbf{s}_b$ ,  $\mathbf{A}_s$  can be specified as an orthogonal spatial basis function of  $\mathbf{s}$ . A natural choice is to let  $\mathbf{A}_s$  be the eigenvectors corresponding to the largest  $d$  eigenvalues in the eigendecomposition of the correlation matrix  $\mathbf{R}_s$ , where the  $(i, j)$ th entry is specified by a kernel function  $K_s(\mathbf{s}_i, \mathbf{s}_j)$ , for  $1 \leq i, j \leq n_1$ . This approach is different than Gu and Shen (2020), where the maximum marginal likelihood estimator of the factor loading matrix was derived and used in the analysis, without taking into account the spatial correlation of the output over input  $\mathbf{s}$ .

We give a few examples of models that can be written as special cases of the GOLF model with certain choice of the latent factor loading matrix. For simplicity, we assume the mean is zero. The first and second classes of models are the GP models with separable covariance functions of input with two dimensions and three dimensions, respectively.

**Example 1** (Spatial model with separable covariance). Consider a spatial model of  $\mathbf{Y}$  at a regular  $n_1 \times n_2$  lattice, where the  $(i, j)$ th input is  $(s_i, x_j)$  with  $s_i$  and  $x_j$  denoting the  $i$ th latitude coordinate and  $j$ th longitude coordinate, respectively. Assume the covariance of the spatial process is separable, meaning that  $\mathbf{Y} \sim \mathcal{N}(\mathbf{0}, \sigma^2 \mathbf{R}_s \otimes \mathbf{R}_x + \sigma_0^2 \mathbf{I}_{n_1 n_2})$ , where the  $(l_1, m_1)$  term of  $\mathbf{R}_s$  is parameterized by the kernel function  $K_s(s_{l_1}, s_{m_1})$  and the  $(l_2, m_2)$  term of  $\mathbf{R}_x$  is  $K_x(x_{l_2}, x_{m_2})$  for  $1 \leq l_1, m_1 \leq n_1$  and  $1 \leq l_2, m_2 \leq n_2$ . Let  $\mathbf{R}_s = \mathbf{U}_s \boldsymbol{\Lambda}_s \mathbf{U}_s^T$ , where  $\mathbf{U}_s$  is a matrix of eigenvectors and  $\boldsymbol{\Lambda}_s$  is a diagonal matrix of eigenvalues of  $\mathbf{R}_s$  with the  $l$ th



diagonal term  $\lambda_l$ . The density of this spatial model is equivalent to model (1) with  $\mathbf{A}_s = \mathbf{U}_s$ ,  $\Sigma_l = \sigma^2 \lambda_l \mathbf{R}_x$  and  $d = n_1$ .

**Example 2** (Spatio-temporal model with separable covariance). Consider a spatio-temporal model of  $\mathbf{Y}$  at  $n_{1,1} \times n_{1,2} \times n_2$  lattice, where the  $(i, j, k)$ th input is  $(s_{1,i}, s_{2,j}, x_k)$ , with  $s_{1,i}$  and  $s_{2,j}$  denoting the  $i$ th latitude coordinate and  $j$ th longitude coordinate, respectively, and  $x_k$  denoting the  $k$ th time point. Let  $n_1 = n_{1,1} \times n_{1,2}$ . Assume the covariance of the spatio-temporal process is separable, meaning that  $\mathbf{Y} \sim \mathcal{N}(0, \sigma^2 \mathbf{R}_{s_1} \otimes \mathbf{R}_{s_2} \otimes \mathbf{R}_x + \sigma_0^2 \mathbf{I}_{n_1 \times n_2})$  with the  $(l_i, m_i)$ th term of  $\mathbf{R}_{s_i}$  parameterized by the kernel function  $K_s(s_{l_i}, s_{m_i})$  with  $1 \leq l_i, m_i \leq n_{1,i}$  for  $i = 1, 2$ , and the  $(l_3, m_3)$ th term of  $\mathbf{R}_x$  being  $K_x(x_{l_3}, s_{m_3})$  with  $1 \leq l_3, m_3 \leq n_2$ . Let  $\mathbf{R}_{s_i} = \mathbf{U}_i \mathbf{\Lambda}_i \mathbf{U}_i^T$  where  $\mathbf{U}_i$  is a matrix of eigenvectors and  $\mathbf{\Lambda}_i$  is a diagonal matrix of eigenvalues  $\lambda_{l_i}$  for  $1 \leq l_i \leq n_{1,i}$  and  $i = 1, 2$ . The density function of this spatio-temporal model is equivalent to model (1) with  $\mathbf{A}_s = \mathbf{U}_1 \otimes \mathbf{U}_2$ ,  $\Sigma_l = \sigma^2 \lambda_{l_1} \lambda_{l_2} \mathbf{R}_x$  with  $1 \leq l_i, m_i \leq n_{1,i}$  for  $i = 1, 2$ ,  $l = l_1 + (l_2 - 1)n_{1,2}$  and  $d = n_1$ .

The separable covariance is widely used in the emulating and calibrating computationally expensive computer models with scalar output (Sacks et al., 1989; Bayarri et al., 2009) and vector output (Conti and O'Hagan, 2010; Paulo et al., 2012), whereas the isotropic covariance, i.e. the covariance as a function of Euclidean distance of inputs is used more often in modeling spatially correlated data (Gelfand et al., 2010). Note the model of GOLF processes in (1) does not assume separability, as the variance and kernel parameters of each factor processes  $z_l(\cdot)$  can be different. The different kernels of the factor processes make the model more flexible, as the factor processes corresponding to large eigenvalues are often found to be smoother than the ones corresponding to small eigenvalues. The separable covariance may be restrictive in this regard as the factor processes are assumed to have the same kernel and parameters. Other anisotropic kernels, such as the geometrically anisotropic kernel, were studied in Zimmerman (1993) for modeling spatially correlated observations.

We intend to write these spatial or spatio-temporal models as a special case of the GOLF processes for the computational reason. As shown in Equation (4), for data observed on lattice, the likelihood of the GOLF processes can be decomposed into a product of densities on the projected output with lower dimensional input. This decomposition allows us to use some well-developed computational approaches to efficiently compute the likelihood function and to make predictions without approximation. These issues will be discussed in Section 3.2.

One can further reduce the computational complexity by selecting  $d$  eigenvectors corresponding to the  $d$  largest eigenvectors from the eigendecomposition of the correlation matrix  $\mathbf{R}_s$ . The proportion of summation of the  $d$  largest eigenvalues over the summation of total eigenvalues shall be chosen as large as possible, to allow the model to explain the most variability of the signal (Higdon et al., 2008). We found that using more factors than the truth typically will not incur large reduction of predictive accuracy, whereas using much smaller number of factors than the truth will cause a large predictive error (Example 4 in simulated studies). Thus one should be cautious to use very small number of factors.

## 2.4 Kernel functions

We first discuss the kernel function for the factor process  $Z_l(\cdot)$ ,  $l = 1, \dots, d$ . For a function with a  $p_2$ -dimensional input, we assume a product kernel between the inputs (Sacks et al., 1989), i.e. for any input  $\mathbf{x}_a = (x_{a1}, \dots, x_{ap_2})$  and  $\mathbf{x}_b = (x_{b1}, \dots, x_{bp_2})$ ,  $K_l(\mathbf{x}_a, \mathbf{x}_b) = \prod_{i=1}^{p_2} K_{l,i}(|x_{ai} - x_{bi}|)$ , where  $K_{l,i}(\cdot)$  is a kernel of the  $l$ th coordinate of the input for  $l = 1, \dots, d$  and  $i = 1, \dots, p_2$ . We focus on Matérn kernel in this work:

$$K_{l,i}(|x_{ai} - x_{bi}|) = \frac{1}{2^{\nu_{l,i}-1} \Gamma(\nu_{l,i})} \left( \frac{\sqrt{2\nu_{l,i}} |x_{ai} - x_{bi}|}{\gamma_{l,i}} \right)^{\nu_{l,i}} \mathcal{K}_{l,i} \left( \frac{\sqrt{2\nu_{l,i}} |x_{ai} - x_{bi}|}{\gamma_{l,i}} \right),$$

where  $\Gamma(\cdot)$  is the gamma function and  $\mathcal{K}_{l,i}(\cdot)$  is the modified Bessel function of the second kind with a positive roughness parameter  $\nu_{l,i}$  and a nonnegative range parameter  $\gamma_{l,i}$  for  $l = 1, \dots, d$  and  $i = 1, \dots, p_2$ . The roughness parameter of the Matérn kernel controls the smoothness of the process. When  $\nu_{l,i} = \frac{1}{2}$ , the Matérn kernel becomes the exponential kernel:  $K_{l,i}(|x_{ai} - x_{bi}|) = \exp(-|x_{ai} - x_{bi}|/\gamma_{l,i})$ , and when  $\nu_{l,i} \rightarrow \infty$ , the Matérn kernel becomes the Gaussian kernel:  $K_{l,i}(|x_{ai} - x_{bi}|) = \exp(-|x_{ai} - x_{bi}|^2/(2\gamma_{l,i}^2))$ . The half-integer Matérn kernel (i.e.  $(2\nu_{l,i} + 1)/2 \in \mathbb{N}$ ) has a closed form expression. When  $\nu_{l,i} = 5/2$ , for example, the Matérn kernel is

$$K_{l,i}(|x_{ai} - x_{bi}|) = \left( 1 + \frac{\sqrt{5}|x_{ai} - x_{bi}|}{\gamma_{l,i}} + \frac{5|x_{ai} - x_{bi}|^2}{3\gamma_{l,i}^2} \right) \exp \left( -\frac{\sqrt{5}|x_{ai} - x_{bi}|}{\gamma_{l,i}} \right), \quad (9)$$

for  $l = 1, \dots, d$  and  $i = 1, \dots, p_2$ .

In constructing GOLF processes, we decompose the density of the GP model with multi-dimensional input into a product of the orthogonal components with lower dimensional input. This is because the likelihood and the predictive distribution of a GP model with a half-integer Matérn covariance can be computed through linear operations with respect to the sample size by the continuous-time Kalman filter (Särkkä and Hartikainen, 2012), when  $p_2 = 1$ . Due to this reason, we use the Matérn kernel for demonstration purposes. The computational advantage will be discussed in Section 3.2.

For the factor loading matrix, we let  $\mathbf{A}_s$  be the first  $d$  eigenvectors of  $\mathbf{R}_s$ . The kernel functions for  $\mathbf{R}_s$  can be chosen similarly as the kernel for the latent factor processes. Without the loss of generality, we assume  $\mathbf{R}_s$  is parameterized by a product kernel with the range parameters  $\gamma_0$ , and the Matérn kernel being used for each coordinate of  $\mathbf{s}$ .

## 3 Posterior sampling for GOLF processes

### 3.1 A Markov chain Monte Carlo approach

In many applications, the observations contain missing values. Denote  $\mathbf{Y}_v^o$  and  $\mathbf{Y}_v^u$  the vectors of observed data and missing data in matrix  $\mathbf{Y}$  with size  $N_o$  and  $N_u$ , respectively. Directly computing the likelihood includes calculating the inverse and determinant of an  $N_o \times N_o$  covariance matrix, which has computational operations  $O(N_o^3)$  in general, making it infeasible for large number of observations.

Here we discuss a computationally feasible way for the GOLF model when observations are from an incomplete matrix or array. The algorithm is based on orthogonal decomposition of the likelihood function in equation (4) and the posterior independence of the latent factors in Corollary 1.

We start with a set of initial values at the locations with missing observations. Denote  $\mathbf{Y}_v^{(t)} = \text{vec}(\mathbf{Y}^{(t)}) = [(\mathbf{Y}_v^o)^T, (\mathbf{Y}_v^{u,(t)})^T]^T$  an  $N$ -vector, where  $\mathbf{Y}_v^o$  and  $\mathbf{Y}_v^{u,(t)}$  are vectors of observations and samples at the missing locations in the  $t$ th iteration,  $t = 1, \dots, T$ . First, we use a Metropolis algorithm to sample  $\boldsymbol{\Theta}^{(t+1)}$  from the marginal posterior distribution  $p(\boldsymbol{\Theta} \mid \mathbf{Y}^{(t)})$ , where the marginal density is given in Equation (4). In the second step, we sample  $\mathbf{Z}_l^{(t+1)}$  from  $p(\mathbf{Z}_l \mid \mathbf{Y}^{(t)}, \boldsymbol{\Theta}^{(t+1)})$  by Equation (5) for  $l = 1, \dots, d$ , and then we generate  $\mathbf{Y}^{(t+1)} = \mathbf{A}^{(t+1)}\mathbf{Z}^{(t+1)} + \mathbf{E}^{(t+1)}$ , where  $\mathbf{E}^{(t+1)}$  is an  $n_1 \times n_2$  matrix of white noise with variance  $\sigma_0^{(t+1)}$  and  $\mathbf{A}^{(t+1)}$  is a  $n_1 \times d$  matrix of the  $d$  eigenvectors corresponding to the  $d$  largest eigenvalues from the eigendecomposition of the correlation matrix  $\mathbf{R}_s$  in the  $(t+1)$ th iteration. We can obtain  $\mathbf{Y}_v^{u,(t+1)}$  by the last  $N_u$  terms in  $\mathbf{Y}_v^{(t+1)}$ , for  $t = 1, \dots, T$ . Note that the observed data  $\mathbf{Y}_v^o$  is never changed.

For computational reasons, we define the nugget parameter in each kernel (i.e. the inverse of the signal variance to the noise variance ratio parameter)  $\eta_l = \sigma_0^2/\sigma_l^2$  for  $l = 1, 2, \dots, d$ , and the inverse range parameter  $\beta_{l,i} = 1/\gamma_{l,i}$ , where  $i = 1, \dots, p_1$  when  $l = 0$ , and  $i = 1, \dots, p_2$  when  $l \geq 1$ . The transformed parameters  $\tilde{\boldsymbol{\Theta}}$  contain the mean parameters  $\mathbf{B}$ , inverse range parameters  $\boldsymbol{\beta} = (\boldsymbol{\beta}_0, \dots, \boldsymbol{\beta}_d)$ , nugget parameters  $\boldsymbol{\eta} = (\eta_1, \dots, \eta_d)$  of the factor processes and the variance of the noise  $\sigma_0^2$ .

For the mean and noise variance parameters, we use an objective prior  $\pi^R(\mathbf{B}, \sigma_0^2) \propto 1/\sigma_0^2$ . We assume the jointly robust (JR) prior for the kernel parameters:  $\pi^{JR}(\boldsymbol{\beta}_l, \eta_l) \propto (\sum_{i=1}^{p_2} (c_{l,2}\beta_{l,i} + \eta_l))^{c_{l,1}} \exp(-c_{l,3} \sum_{i=1}^{p_2} (c_{l,1}\beta_{l,i} + \eta_l))$  with default parameters  $c_{l,1} = 1/2 - p_2$ ,  $c_{l,2} = 1/2$ , and  $c_{l,3}$  being the average distance between the  $l$ th coordinate of two inputs for  $l = 1, \dots, d$  (Gu, 2018). The jointly robust prior is equivalent to the inverse gamma prior when the input dimension is one without a nugget parameter. The inverse gamma prior is assumed for each coordinate of  $\boldsymbol{\beta}_0$  with shape and rate parameter being  $-1/2$  and  $1$ , respectively. Note here  $c_{l,1} = 1/2 - p_2$  is the default parameter for the MCMC algorithm, whereas this prior parameter is different if one maximizes the marginal posterior distribution. The JR prior can alleviate the potential numerical problem when the estimated range and nugget parameters are close to the boundary of the parameter space, as the density of the JR prior is close to zero at these scenarios. As the sample size is large, the bias inserted from the prior is small.

The MCMC algorithm of the GOLF model is given in Algorithm 1. In the step (1) to step (4) of Algorithm 1, we marginalize out the factor processes to compute the posterior distribution of the parameters. This is critically important as we found severe identifiability problems between the mean matrix  $\mathbf{M}$  and  $\mathbf{AZ}$ , if the parameters are sampled from the full conditional distributions. Moreover, after marginalizing out the factor processes, the covariance matrix of the distribution  $\mathcal{PN}(\tilde{\mathbf{y}}_l; \mathbf{0}, \tilde{\boldsymbol{\Sigma}}_l)$  in (4) contains a nugget term, which makes the computation stable.

The Algorithm 1 can be easily modified for different scenarios. When the factor processes have the same covariance matrix, we can combine step (1) and step (2) to sample the shared kernel and nugget parameter. Step (4) may be skipped if one has zero-mean, or modified if

---

**Algorithm 1** MCMC algorithm when the kernel parameters are different

---

- (1) For  $l = 1, \dots, d$ , sample  $(\beta_l^{(t+1)}, \eta_l^{(t+1)})$  from  $p(\beta_l, \eta_l \mid \tilde{\mathbf{y}}_l^{(t)})$ .
  - (2) Sample  $\beta_0^{(t)}$  from  $p(\beta_0^{(t)} \mid \mathbf{Y}^{(t)}, \beta_{1:d}^{(t+1)}, \eta_{1:d}^{(t+1)}, \mathbf{B}^{(t)})$ .
  - (3) Sample  $\sigma_0^{(t+1)}$  from  $p(\sigma_0^{(t+1)} \mid \mathbf{Y}^{(t)}, \beta^{(t+1)}, \eta^{(t+1)}, \mathbf{B}^{(t)})$ .
  - (4) Sample  $\mathbf{B}^{(t+1)}$  from  $p(\mathbf{B} \mid \mathbf{Y}^{(t)}, \beta^{(t+1)}, \eta^{(t+1)})$ . Update the mean matrix  $\mathbf{M}^{(t+1)}$  and the projected observations  $\tilde{\mathbf{y}}_l^{(t)} = (\mathbf{Y} - \mathbf{M}^{(t+1)})^T \mathbf{a}_l$ .
  - (5) For  $l = 1, \dots, d$ , sample  $(\mathbf{Z}_l^{(t+1)})^T$  from  $p(\mathbf{Z}_l^T \mid \tilde{\mathbf{y}}_l^{(t)}, \beta^{(t+1)}, \eta^{(t+1)})$  by Corollary 1 and sample  $\mathbf{Y}^{(t+1)}$  by model (1). Update  $\mathbf{Y}_v^{u,(t+1)}$  by the last  $N_u$  terms in  $\mathbf{Y}_v^{(t+1)}$  and let  $\tilde{\mathbf{y}}_l^{(t+1)} = (\mathbf{Y}^{(t+1)} - \mathbf{M}^{(t+1)})^T \mathbf{a}_l$ .
  - (6) Update the posterior  $p(\beta_l^{(t+1)}, \eta_l^{(t+1)} \mid \tilde{\mathbf{y}}_l^{(t+1)})$  and go back to (1) when  $t < T$ .
- 

one has the shared regression coefficients in the model.

Denote  $\Sigma_l = \mathbf{L}_l \mathbf{L}_l^T$  where  $\mathbf{L}_l$  is a lower triangular matrix in the Cholesky decomposition of  $\Sigma_l$ . We need to efficiently compute the terms  $|\tilde{\Sigma}_l|$ ,  $\mathbf{L}_l^{-1} \mathbf{v}_l$ ,  $\mathbf{L}_l \mathbf{v}_l$  for any real-valued vector  $\mathbf{v}_l := (v_{l,1}, \dots, v_{l,n_2})^T$  and sample  $(\mathbf{Z}_l^{(t+1)})^T$  from  $p(\mathbf{Z}_l^T \mid \tilde{\mathbf{y}}_l^{(t)}, \beta^{(t+1)}, \eta^{(t+1)})$  for  $l = 1, \dots, d$ . Direct computation of the Cholesky decomposition or the determinant of  $\Sigma_l$  requires  $O(n_2^3)$  computational operations for each  $l = 1, \dots, d$ . Luckily, for Matérn covariance with half-integer roughness parameter and one-dimensional input, computing any of these terms through the continuous-time Kalman filter only takes  $O(n_2)$  computational operations without any approximation. This algorithm is introduced in Section 3.2, and the computational complexity is discussed in Section 3.3.

### 3.2 Continuous-time Kalman filter

We briefly review the continuous-time Kalman filter algorithm here. The connection between the Gaussian Markov random field and Gaussian random field with a Matérn covariance function was explored in previous studies. In Whittle (1954, 1963); Hartikainen and Sarkka (2010), the spectral density of the Matérn kernel with the half-integer roughness parameter is shown to be the same as a continuous time autoregressive process defined as a stochastic differential equation (SDE). Suppose the observations are  $\tilde{\mathbf{y}}_l = (\tilde{y}_{l,1}, \dots, \tilde{y}_{l,n_2})^T$ . For  $j = 1, \dots, n_2$  and  $l = 1, \dots, d$ , starting from the initial state  $\boldsymbol{\theta}_l(s_0) \sim \text{MN}(\mathbf{0}, \mathbf{W}_l(s_0))$ , the solution of the SDE can be written as a continuous-time dynamic linear model (Hartikainen and Sarkka, 2010):

$$\begin{aligned} \tilde{y}_{l,j} &= \mathbf{F} \boldsymbol{\theta}_l(x_j) + \epsilon_{l,j}, \\ \boldsymbol{\theta}_l(x_j) &= \mathbf{G}_l(x_{j-1}) \boldsymbol{\theta}_l(x_{j-1}) + \mathbf{w}_l(x_j), \end{aligned} \tag{10}$$

where  $\mathbf{w}_l(x_j) \sim \mathcal{N}(\mathbf{0}, \mathbf{W}_l(s_j))$ ,  $\epsilon_{l,j}$  is an independent white noise for  $l = 1, \dots, d$  and  $j = 1, \dots, n_2$ . For the Matérn kernel with a half-integer roughness parameter, the terms  $\mathbf{G}_l(x_j)$ ,  $\mathbf{W}_l(x_j)$ , and  $\mathbf{F}$  can be expressed explicitly as a function of  $|x_j - x_{j-1}|$  and the range parameter of the kernel. Thus, the forward filtering and backward smoothing algorithm (FFBS) can be applied to compute the likelihood and to make predictions with linear computational operations of the number of observations (see e.g. Chapter 4 in West and Harrison (1997)

and Chapter 2 in Petris et al. (2009) for the FFBS algorithm). The closed form expressions of  $\mathbf{G}_l(x_j)$ ,  $\mathbf{W}_l(x_j)$ , and  $\mathbf{F}$  for Matérn kernel in (9) and the FFBS algorithm are discussed in Gu and Xu (2020). The likelihood function and predictive distribution of a GP model having the Matérn kernel with roughness parameters being 1/2 and 5/2 through the FFBS algorithm are implemented in **FastGaSP** package available at CRAN. The key advantage of the FFBS algorithm is that the computational operation is only  $O(n_2)$  with  $n_2$  being the number of observations, instead of  $O(n_2^3)$  required in computing the Cholesky decomposition of the covariance matrix.

We briefly discuss how to apply the FFBS algorithm to compute the terms  $\mathbf{L}_l^{-1}\tilde{\mathbf{y}}_l$  and  $|\tilde{\Sigma}_l|$  needed in Algorithm 1, for  $l = 1, \dots, d$ . In the FFBS algorithm, the one-step-ahead predictive distribution  $(\tilde{y}_{l,j} \mid \tilde{y}_{l,1:j-1}) \sim \mathcal{N}(f_l(x_j), Q_l(x_j))$  can be derived iteratively for  $j = 1, \dots, n_2$  and for each  $l = 1, \dots, d$ . Closed form expressions of  $f_l(x_j)$  and  $Q_l(x_j)$  for the Matérn covariance in (9) are given in Gu and Xu (2020). For  $l = 1, \dots, d$ , we have following expressions for the computational expensive terms in the likelihood function:

$$|\tilde{\Sigma}_l| = \prod_{j=1}^{n_2} Q_l(x_j), \quad \text{and} \quad \mathbf{L}_l^{-1}\tilde{\mathbf{y}}_l = \left( \frac{\tilde{y}_{l,1} - f_{l,1}}{\sqrt{Q_l(x_1)}}, \dots, \frac{\tilde{y}_{l,1} - f_{l,n_2}}{\sqrt{Q_l(x_{n_2})}} \right)^T.$$

We use the backward sampling algorithm (Petris et al., 2009) to sample  $\boldsymbol{\theta}_{l,n_2}$  from  $p(\boldsymbol{\theta}_{l,n_2} \mid \tilde{\mathbf{y}}_l^{(t)}, \boldsymbol{\beta}^{(t+1)}, \boldsymbol{\eta}^{(t+1)})$  and  $\boldsymbol{\theta}_{l,j}$  from  $p(\boldsymbol{\theta}_{l,j} \mid \tilde{\mathbf{y}}_l^{(t)}, \boldsymbol{\theta}_{l,j+1}, \boldsymbol{\beta}^{(t+1)}, \boldsymbol{\eta}^{(t+1)})$  sequentially, for  $j = n_2 - 1, \dots, 1$ . The posterior sample  $\mathbf{Z}_l^T = (\mathbf{z}_l(x_1), \dots, \mathbf{z}_l(x_{n_2}))^T$  can be obtained by the first entry of posterior sample  $\boldsymbol{\theta}_{l,j}$  from the backward sampling algorithm, for  $j = 1, \dots, n_2$ . Furthermore, for any  $n_2 \times 1$  real vector  $\mathbf{v}_l$ , we have  $\mathbf{L}_l\mathbf{v}_l = (f_{l,1} + \sqrt{Q_l(x_1)}v_{l,1}, \dots, f_{l,n_2} + \sqrt{Q_l(x_{n_2})}v_{l,n_2})^T$  for  $l = 1, \dots, d$  and  $j = 1, \dots, n_2$ . We use these computationally feasible ways to compute the required quantities so the computational complexity is linear with respect the number of observations ( $n_2$ ).

### 3.3 Computational complexity

Denote  $p = p_1 \times p_2$  the total dimension of the inputs  $(\mathbf{s}, \mathbf{x})$  and suppose the observational matrix is  $n_1 \times n_2$  with irregular missing values, where  $n_1 \leq n_2$  and  $N = n_1 n_2$ . We discuss the computational complexity for three scenarios with  $p = 2$  (e.g. spatially correlated data),  $p = 3$  (e.g. spatio-temporal data) and  $p > 3$  (e.g. functional data).

For the case when  $p = 2$ , the computational operations are  $O(Nd)$  for the GOLF model with the half-integer Matérn kernel and mean pattern listed in Table 1. First to obtain  $\mathbf{A}_s$ , we compute the first  $d$  eigenvectors of  $\Sigma_s$ , which has  $O(n_1^2 d)$  operations (see e.g. Chapter 4.5.5 in Bai et al. (2000)). Second, computing the marginal likelihood and sampling the factor processes by the FFBS algorithm only cost  $O(n_2 d)$  operations. The largest computational order is from the matrix multiplication  $\tilde{\mathbf{Y}}^T = (\mathbf{Y} - \mathbf{M})^T \mathbf{A}_s$ , which is at the order of  $O(Nd)$ .

For the case when  $p = 3$ , we let  $\mathbf{A}_s = \mathbf{A}_{s_1} \otimes \mathbf{A}_{s_2}$ , where  $\mathbf{A}_{s_1}$  and  $\mathbf{A}_{s_2}$  are the first  $d_1$  and  $d_2$  eigenvectors of  $n_{1,1} \times n_{1,1}$  matrix  $\Sigma_{s_1}$  and  $n_{1,2} \times n_{1,2}$  matrix  $\Sigma_{s_2}$ , respectively, with  $n_{1,1} \times n_{1,2} = n_1$  and  $\Sigma_{s_1} \otimes \Sigma_{s_2} = \Sigma_s$ . Without the loss of generality, assume  $d_1 \leq d_2$  and  $n_1 \leq n_2$ . Let the total number of factor processes be  $d = d_1 d_2$ . The computational order of the GOLF model with a half-integer Matérn covariance function is  $O(n_1 n_2 d_{\max})$  with  $d_{\max}$  being the maximum of  $d_1$  and  $d_2$  (noting this is much smaller than  $O(n_1 n_2 d)$ ). To see this, computing the

eigendecomposition of  $\Sigma_{s_1}$  and  $\Sigma_{s_2}$  requires  $O(d_1 n_{1,1}^2)$  and  $O(d_2 n_{1,2}^2)$  operations, respectively. Second, using the FFBS algorithm to compute the marginal likelihood and to sample factor processes costs  $O(dn_2)$  operations. At last, we do NOT directly compute  $\mathbf{Y}^T \mathbf{A}_s$  as its computation operations are  $O(Nd)$ . Instead, we first write the observations as an  $n_2 \times n_{1,2} \times n_{1,1}$  array  $\mathbf{Y}_{ar}^T$ , where the  $(i, j, k)$ th entry being the outcome at  $(s_{1,i}, s_{2,j}, x_k)$ . Then we do a 3-mode matrix product followed by a 2-mode matrix product  $\tilde{\mathbf{Y}}_{ar}^T \times_3 \mathbf{A}_{s_1} \times_2 \mathbf{A}_{s_2}$  (Kolda and Bader, 2009), which has the computation operations  $O(n_2 n_1 d_1)$  and  $O(n_2 n_{1,2} d)$ , respectively. Finally we concatenate the second and third dimensions of  $\tilde{\mathbf{Y}}_{ar}^T$  to obtain the  $n_2 \times d$  matrix  $\tilde{\mathbf{Y}}^T$ .

For the case when  $p > 3$ , there might be two scenarios. In the first scenario, the data are observed in an  $n_{1,1} \times n_{1,2} \times \dots \times n_{1,k} \times n_2$  tensor with irregular missing values, where  $n_{1,1} \times n_{1,2} \times \dots \times n_{1,k} = n_1$ . In this scenario, the computation will be  $Nd_{max}$ , where  $d_{max}$  is the maximum of  $d_1, \dots, d_k$  with similar deduction for the case with  $p = 3$ . In the second scenario, we have  $p_2 > 1$ . Examples include emulating a computationally expensive computer output with multivariate output (Conti and O'Hagan, 2010; Paulo, 2005). In this case, the Kalman filter algorithm may not be applied, so the additional computational order is  $O(n_2^3)$ , when the covariance of the factor process is the same. If the covariance is not the same, we need to additionally compute the inverse of covariance matrices of  $d$  multivariate normal distributions, which is at the order of  $O(dn_2^3)$ .

In sum, when data are from incomplete matrices or arrays, the computation in each step of MCMC algorithm is  $O(Nd)$  for  $p_2 = 2$  or  $O(Nd_{max})$  for  $p_2 > 2$ , which is much better than  $O(N_0^3)$  from directly inverting the covariance matrices. Besides, a few steps in the MCMC algorithm can be computed in parallel, such as FFBS algorithm to compute the product of  $d$  marginal densities of projected output and the matrix multiplication  $\tilde{\mathbf{Y}}^T = (\mathbf{Y} - \mathbf{M})^T \mathbf{A}_s$ , to further reduce the computational complexity.

## 4 Comparison and connection with other related models

GOLF processes are closely connected to a wide range of approaches on approximating Gaussian process for modeling large correlated data. Model (1) is a special case of linear model of coregionalization (LMC) (Gelfand et al., 2004), where the factor loading matrix is allowed to change along with the input in the latent processes. The LMC is more flexible, yet more computationally intensive than our model. Another widely used model for multivariate functional data is the semiparametric latent factor model (SLFM) (Seeger et al., 2005), where the factor loading matrix can be estimated by the principal component analysis (PCA) (Higdon et al., 2008) or the GPPCA (Gu and Shen, 2020). Our approach has two distinctions. First, the observations are often required to be a matrix or an array in SLFM, whereas our approach applies to incomplete matrix or array observations with missing values. Second, both input  $\mathbf{s}$  and input  $\mathbf{x}$  are used for estimation, whereas only the input in latent processes ( $\mathbf{x}$ ) is used in PCA or GPPCA for the SLFM. When the latent function has input  $\mathbf{s}$  and  $\mathbf{x}$ , our estimation can lead to more accurate prediction of missing values.

Our primary motivation is on projecting the observations on orthogonal coordinates to

overcome the computational bottleneck of GPs, as the complexity of computing likelihood with Matérn covariances with one dimension input is linear to the number of observations by the continuous time Kalman Filter. For an  $n_{1,1} \times n_{1,2} \times \dots \times n_{1,k} \times n_2$  incomplete array observations, the computational operations of the likelihood are  $O(Nn_{1,max})$  without reducing the rank of the covariance, where  $n_{1,max}$  is the maximum of  $n_{1,1}, n_{1,2}, \dots, n_{1,k}$ , which is much smaller than  $O(N^3)$ , with  $N = n_{1,1} \times n_{1,2} \times \dots \times n_{1,k} \times n_2$ . The computational complexity can be further reduced by using factor processes corresponding to large eigenvalues. The reduced rank approach is used widely in modeling spatially correlated data. For instance, the predictive process by a set of pre-specified knots was studied in Banerjee et al. (2008), and the multiresolution local bisquare functions were used in Cressie and Johannesson (2008). Limitations of reduced-rank method are studied in Stein (2014). We find in simulation that using much smaller number of factors than the truth may cause a large predictive error, indicating that one should not reduce the rank of covariance if computation allows.

Many other approximation methods for GPs follow the framework of the Vecchia’s approximation (Katzfuss and Guinness, 2017; Vecchia, 1988), where the likelihood of the latent process is approximated by a product of conditional densities (conditioning on prespecified random vectors in the parental index set). A few widely used approaches, such as the hierarchical nearest neighboring Gaussian processes (NNGP) (Datta et al., 2016), dynamic linear models (Petrus et al., 2009), multi-resolution approximation (MRA) (Katzfuss, 2017) and full-scale approximation Sang and Huang (2012), can be written as Vecchia’s approximation. GOLF processes developed herein can also be viewed as a special case of Vecchia’s approximation when Matérn kernel is used, in a sense that the model can be written as a vector autoregressive model with orthogonal factor loading matrix (Prado and West, 2010). Vecchia’s approximation is a broad framework that essentially assumes the sparsity of the inverse of Cholesky decomposition of the covariance matrix of the latent processes. The key of Vecchia’s approximation is on selecting the order of the latent variables and imposing sensible conditional independence assumptions between variables. We compare our approach with a few other methods that fall into the framework of the Vecchia’s approximation in Section 6.1.

## 5 Simulated studies

We discuss two simulated examples in this section. We first study a simulated example with a small sample size, where the data are generated from the separable Gaussian process in Example 1 with different missing patterns. We compare the predictive performance and parameter inference between GOLF processes and the exact GP model by directly computing the inversion and determinant of the covariance matrix in the likelihood function. In the second simulated example, we generate the observations from the separable model and non-separable model to study the predictive performance of the GOLF processes with different number of factors, shared and different kernel parameters. For both examples, we implement  $J = 100$  experiments in each scenario and we generate  $T = 5,000$  MCMC samples for each method with the first 20% of the samples used as the burn-in samples.

Denote  $y_{i,j}^*$  the  $i$ th held-out data in the  $j$ th simulated experiment in each scenario, for  $i = 1, \dots, n^*$  and  $j = 1, \dots, J$ . Let  $\hat{y}_{ij}^*$  and  $CI_{ij}(95\%)$  be the predictive mean and 95%

predictive credible interval of the  $i$ th held-out data at the  $j$ th experiment, respectively. For both simulated examples, we record the root mean square error, the percentage of held-out observations percentage covered in the 95% predictive interval, and the average length of the 95% predictive interval of the  $j$ th experiment ( $LCI_j(95\%)$ ):

$$\text{RMSE}_j = \sqrt{\frac{\sum_{i=1}^{N^*} (\hat{y}_{ij}^* - y_{ij}^*)^2}{N^*}}, \quad (11)$$

$$P_{CI_j}(95\%) = \frac{1}{N^*} \sum_{i=1}^{N^*} 1\{y_{ij}^* \in CI_{ij}(95\%)\}, \quad (12)$$

$$LCI_j(95\%) = \frac{1}{N^*} \sum_{i=1}^{N^*} \text{length}\{CI_{ij}(95\%)\}, \quad (13)$$

for  $j = 1, \dots, J$ . Then we compute the average values of the these three quantities over  $J = 100$  simulations to evaluate each approach. A precise method should have small average RMSE,  $P_{CI}(95\%)$  close to be 95% and short length of the predictive interval.

**Example 3** (GOLF processes and exact GP model). *The data are sampled from zero-mean separable GP model with two dimensional inputs at a  $25 \times 25$  regular lattice in  $[0, 1]^2$ . Two missing patterns are considered, where the data are missing at random in the first case, and a disk in the centroid of the lattice is missing in the second case.*

We assume a small sample size in Example 3 because of the computational burden by the exact Gaussian process model. We use the unit-variance covariance matrix parameterized by the exponential kernel and the Matérn kernel in (9) to generate the data. The range parameters of Matérn kernel are chosen as  $\gamma_0 = 1$  and  $\gamma_1 = \dots = \gamma_d = 1/3$ . The range parameters of exponential kernel are chosen to be  $\gamma_0 = 4$  and  $\gamma_1 = \dots = \gamma_d = 1$ . All the range parameters, the variance of the kernel and noise are estimated by each method based on the MCMC algorithm.

We compare GOLF processes and the exact GP model where the inverse and determinant of the covariance matrix are directly computed. Both models use the same prior and proposal distribution in the MCMC algorithm to sample the kernel parameters. In Table 2, we give the predictive performance of both methods for three scenarios, where 50% and 20% of the output are missing at random in the first two scenarios, and approximately 20% of the output are missing in a disk in the centroid of the lattice in the third scenario. Graphs of the observed data, full data, predictions and trace plots of the posterior samples in one simulation are given in the supplementary materials.

As shown in Table 2, both methods have accurate predictions and uncertainty assessment for all scenarios. The out of sample RMSE for predicting the held out observations is close to 0.1, the standard deviation of the noise. The 95% predictive confidence intervals cover around 95% of the held-out observations and the average length of the predictive confidence interval is small. The predictions of both methods are more precise for the cases when the data are missing at random than the ones when a disk of output is missing in the centroid of the lattice, as the estimated correlation between the held-out test output and nearby observations are relatively accurate.



Kernel	Missing value		GOLF			Exact GP model			Difference		
	Percentage	Pattern	RMSE	$P_{CI}(95\%)$	$L_{CI}(95\%)$	RMSE	$P_{CI}(95\%)$	$L_{CI}(95\%)$	$\Delta RMSE$	$\Delta L$	$\Delta U$
Matérn	50%	random	0.106	0.954	0.425	0.106	0.952	0.423	0.002	0.006	0.006
	20%	random	0.103	0.952	0.410	0.103	0.952	0.411	0.001	0.007	0.007
	20%	disk	0.108	0.909	0.430	0.108	0.913	0.431	0.005	0.008	0.009
Exp	50%	random	0.129	0.955	0.518	0.128	0.953	0.513	0.005	0.009	0.008
	20%	random	0.120	0.947	0.472	0.120	0.948	0.471	0.003	0.009	0.009
	20%	disk	0.156	0.941	0.602	0.154	0.946	0.605	0.013	0.019	0.019

Table 2: Comparison between the exact GP model and GOLF processes.  $J = 100$  simulated experiments are conducted for each scenario.  $\Delta RMSE = \frac{1}{J} \sum_{j=1}^J \Delta RMSE_j$  measures the average  $L_2$  distance by the two methods, where  $\Delta RMSE_j = (\frac{1}{N^*} \sum_{i=1}^{N^*} (\hat{y}_{ij,GOLF}^* - \hat{y}_{ij,GP}^*)^2)^{1/2}$  with  $\hat{y}_{ij,GOLF}^*$  and  $\hat{y}_{ij,GP}^*$  denote the predictive mean by GOLF processes and exact GP model, respectively.  $\Delta L$  and  $\Delta U$  measure the average absolute difference between the lower bound and upper bound of 95% predictive intervals of the GOLF processes and the exact GP model, respectively.

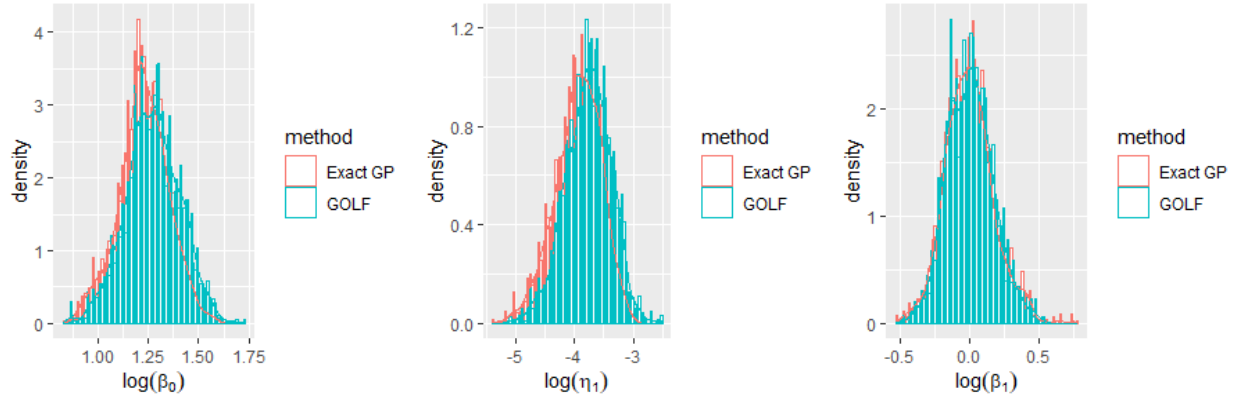


Figure 2: The histogram of posterior samples of the logarithm of the inverse range parameters and nugget parameters in one simulation of Example 3, where the data are generated using the Matérn kernel in (9) with 50% of the values missing at random.

For Example 3, note that GOLF processes and the exact GP model are the same model with two different computational strategies. For GOLF processes, we sample the missing values to use the fast computational strategy for GOLF processes, whereas the inverse and determinant of the covariance matrix are computed in the exact GP model directly. The two different strategies have significantly different computational operations. The computational operations of GOLF processes is  $O(Nd)$  with  $N = n_1 \times n_2$  ( $d = n_1$  in Example 3), whereas the computational operations of the exact GP model is  $O(N_o^3)$ , where  $N_o$  is the number of observations. Thus, GOLF processes are computationally feasible for a large data set. On the other hand, the difference in predictions and uncertainty assessment between the exact GP model and GOLF is small (last three columns in Table 2), since we do not make any approximation in GOLF processes.

Figure 2 shows the histogram of the 4000 after burn-in posterior samples from the GOLF processes and exact GP model in one simulation of Example 3. The posterior samples of two methods are close to each other. The difference becomes even smaller when we increase the number of MCMC samples.

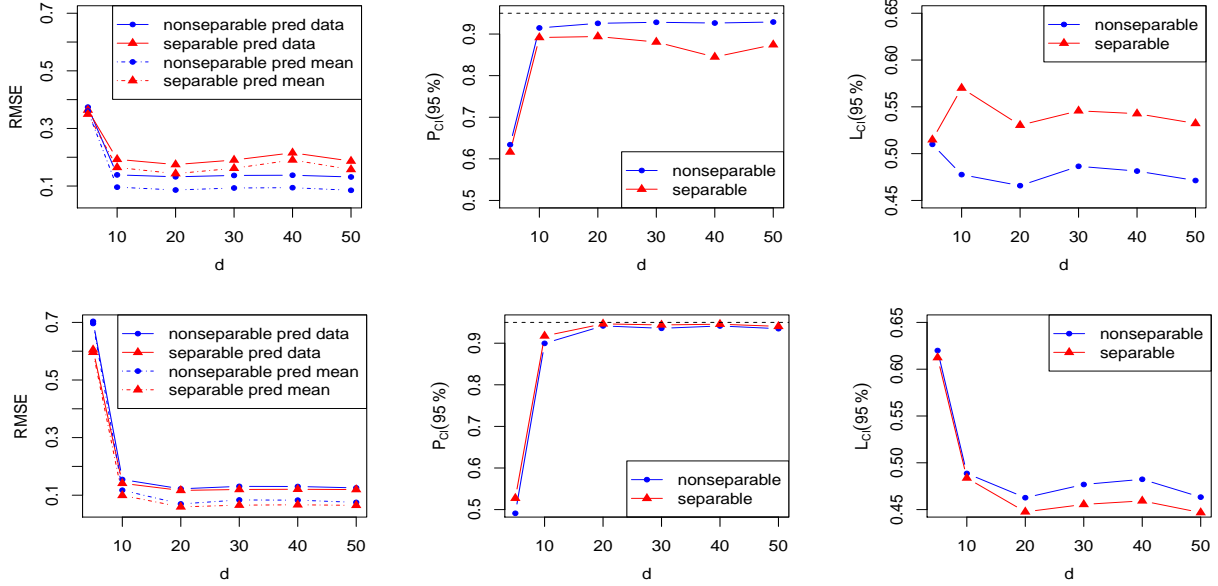


Figure 3: The predictive performance of GOLF process with  $d = 5, 10, 20, 30, 40$  and  $50$  factors for Example 4. The nonseparable kernel with distinct kernel parameters is assumed to generate the data in the first row of panels, and separable kernel with the same kernel parameter of each factor process is used for simulation in the second row of panels. The blue curves and red curves denote the performance by the GOLF processes with the different kernel parameters and the same kernel parameter, respectively. In the left panels, the solid curves denote the RMSE for predicting the (noisy) observations, and the dashed curve denote the RMSE for predicting the mean of the observations. The proportions of observations covered in the 95% predictive interval and the average length of the predictive interval are graphed in the middle and right panels, respectively.

**Example 4** (GOLF processes with different number of factors and kernel parameters). *The data are sampled from two scenarios with two dimensional inputs being a  $100 \times 100$  lattice in  $[0, 1]^2$ . In the first scenario, the range parameters of the kernel of each factor process are the same, whereas these parameters are chosen to be different in the second scenario. In both scenarios, a disk of output in the centroid of the lattice is masked out for testing, corresponding to approximately 20% of the total number of data. We use  $d = 30$  (low-rank) and  $d = 100$  (full-rank) factors to generate the data. We test GOLF processes with different number of factors, same or different range parameters.*

In Example 4, the factor processes are assumed to have the Matérn kernel in (9) and unit variance. The kernel parameter is shared in the first scenario, where  $\gamma_0 = 1/4$  and  $\gamma_l = 1/2$ , and in the second scenario  $\gamma_0 = 1/3$  and  $\gamma_l = 1/l$ , for  $l = 1, \dots, d$ . We estimate these parameters through the posterior samples from the MCMC algorithm.

We graph the predictive RMSE, percentage of output covered in the 95% predictive credible interval and average length of the predictive interval of different approaches in Figure 3, when the true number of factor processes is 30. All results are averaged over

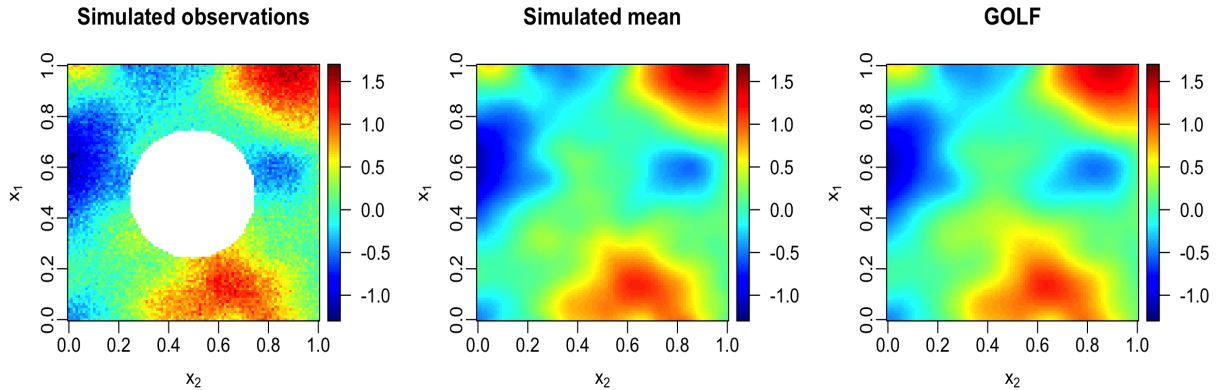


Figure 4: The observed data, the mean of the data, and the prediction from GOLF processes in one simulation of Example 4.

$J = 100$  simulations. In the first row of the panels, since the data are simulated by GOLF processes with different kernel parameters, the nonseparable GOLF processes have smaller predictive RMSE and has a shorter interval that covers almost 95% of the data. In second row of the panels, the GOLF processes with the same kernel parameter seem to be slightly better, as the true factor process has the same kernel parameter. The difference between two methods in the second row is smaller, as the GOLF processes with a separable kernel is a special case of the one with different kernel parameters.

The data are simulated using  $d = 30$  factor processes. From Figure 3, we found that when we use  $d = 20$  factor processes or more, the predictive results seem to be similar. The way of selecting the number of factors is currently ad-hoc. One may select the number of factors to ensure a large proportion of the variance explained by the sum of the eigenvalues of correlation matrix  $\mathbf{R}_s$ . This simulation suggests that using more factors may be better in prediction than using very few factors.

In Figure 4, we graph the simulated observations, simulated mean and the prediction from the GOLF model with  $d = 30$  in one simulation. The predictions indeed look accurate. The predictive performance of different approaches when the data are generated by a full rank kernel ( $d = 100$ ) is given in Figure S2 in supplementary materials. The results are very similar to Figure 3.

## 6 Real applications

### 6.1 Predicting large spatial data on an incomplete lattice

We compare the GOLF processes with different approaches on predicting the missing temperature values in Heaton et al. (2019). This data set contains daytime land surface temperatures on August 4, 2016 at  $300 \times 500$  spatial grids with the latitude and longitude ranging from 34.30 to 37.07, and from -95.91 to -91.28, respectively. The complete data set consists of 148,309 observations with 1,791 missing values due to cloud cover. The training data (plotted in the left panel in Figure 1) consists of 105,569 observations, whereas 42,740

Methods	RMSE	$P_{CI}(95\%)$	$L_{CI}(95\%)$	Run time (mins)
FRK	3.16	0.77	6.09	3.53
Gapfill	1.86	0.35	1.44	6.98
GOLF	1.46	0.92	4.95	48.6
LAGP	2.07	0.84	5.70	3.76
LatticeKrig	1.68	0.963	6.58	214.25
MRA	1.85	0.92	5.54	4.99
NNGP	1.64	0.95	5.84	1.14
Partition	1.80	0.82	4.56	827.37
SPDE	1.55	0.97	7.87	34.8

Table 3: Comparison for the dataset in Heaton et al. (2019). The standard deviation of the outcomes in this dataset is 4.07.

observations were held-out as the test data.

In Heaton et al. (2019), 12 groups of researchers across the globe implemented their methods to predict missing temperature values. Among this cohort of researchers, are authors that conjured up some of the most popular methods for large spatially correlated data. The full data set that contains the held-out values was not released in the competition.

We implement the GOLF model on this dataset with  $s$  being latitude and  $x$  being longitude. For the mean function, we assume a mean parameter for each latitude of the observations due to scientific reasons, i.e.  $\mathbf{M} = (\mathbf{H}_2\mathbf{B}_2)^T$ , where  $\mathbf{H}_2 = \mathbf{1}_{n_2}$  and  $\mathbf{B}_2 = (b_{2,1}, \dots, b_{2,n_1})^T$ . We let  $d = n_1/2$  and assume exponential kernels for both inputs. For each factor process, we assume distinct variances and range parameters sampled from the marginal posterior distribution. We compute  $M = 6000$  posterior samples where the first 20% were used as the burn-in samples. Results of longer MCMC chains and different initial values of the parameters are given in the supplementary materials.

The predictive performance of different approaches are recorded in Table 3. Other than GOLF processes, we implement 8 of 12 approaches based on the code provided in (Heaton et al., 2019). We could not implement the other the four approaches due to either memory limitation of computing facility or unavailability of the code. All computations are operated on a 3.60GHz 8 cores Intel i9 processor with 32 GB of RAM on a macOS Mojave operating system.

The training observations and the full observations are graphed in the upper panel in Figure 5. Predicting the missing values of this data set is challenging, as the observations are missing in different spatial blocks. From Table 3, most of results seem to be consistent with what is shown in Heaton et al. (2019), whereas small difference remains in few methods requiring random starts or a stochastic algorithm. For example, for the SPDE method, we ran 5 times using the provided code from the authors and found the predictive RMSE of each time ranges from 1.55 to 1.88. Besides, the run time seems different, as the computing system is not the same. E.g. for SPDE and LatticeKrig, it takes 35 mins and 214 mins to run in our system, respectively, whereas it takes 138 mins and 78 mins to run in Heaton et al. (2019), respectively.

The GOLF model has the lowest RMSE compared with the other methods. We acknowl-

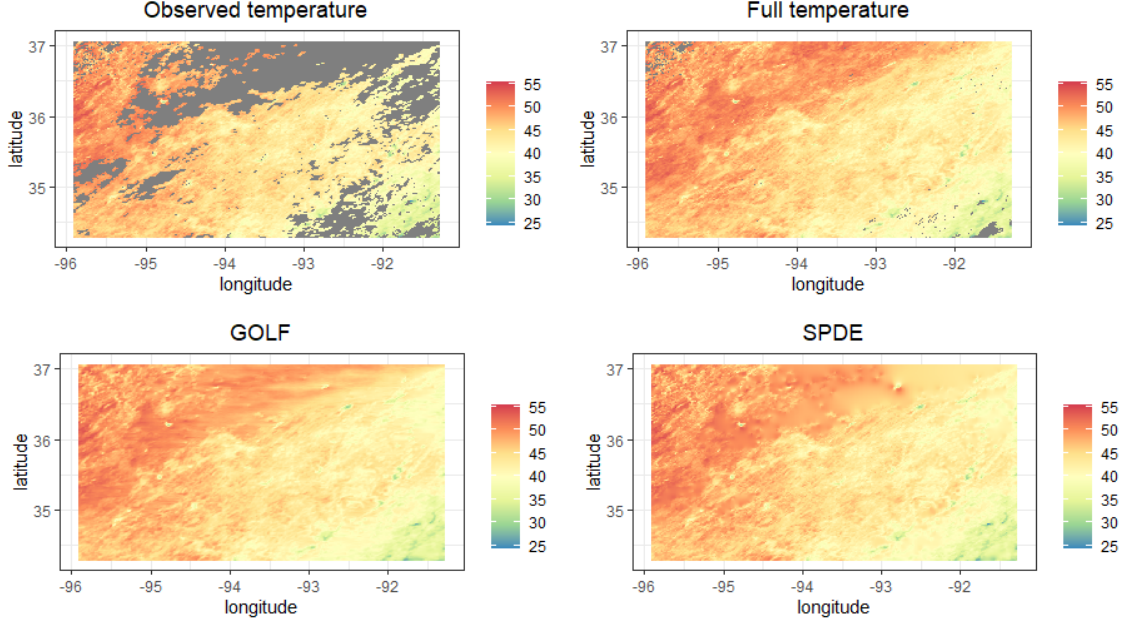


Figure 5: The observed data, full data, predictions from GOLF and from SPDE.

edge that held-out observations were not released in Heaton et al. (2019), whereas we know the held-out observations when implementing the GOLF model. The good performance by the GOLF model may be explained by two reasons. First, we assume different mean parameters for the observations at each latitude and sample these parameters from the marginal posterior distribution in the MCMC algorithm. The distinct mean parameters are more flexible to capture information from a large number of observations. Second, we assume different range and variance parameters of the factor processes, which is more flexible than the separable or isotropic kernel functions.

The 95% predictive interval of the GOLF model is the shortest, and it covers around 92% of the held out test data as shown in Table 3. In supplementary materials, we provide diagnostic plots of the fitted values from the GOLF model, and predictive performance based on several configurations including 40,000 MCMC samples and different initial parameters. The predictive performance of the GOLF model at different configurations is similar. Besides, the computational time of GOLF per one MCMC iteration is around 0.49s for this example. Future works are needed to reduce the number of iterations to achieve similar level of predictive accuracy.

The predictive mean of the GOLF processes and SPDE (the second best method in terms of RMSE) are graphed in middle panel and right panel in Figure 5, respectively. Both methods seem precise in prediction. The prediction from the GOLF processes seems to be more accurate in the northeast region.

## 6.2 Analysis of large spatio-temporal data set

We consider the monthly gridded temperature anomalies from U.S. National Oceanic and Atmospheric Administration (NOAA) in this section. The data set contains the average air and marine temperature across the globe. We compare the predictive performance using the

Methods	RMSE	$P_{CI}(95\%)$	$L_{CI}(95\%)$	Run time (mins)
FRK	0.846	0.967	3.92	29.4
GOLF	0.325	0.942	1.08	43.9
LAGP	0.695	0.951	1.80	6.18
Spatial model 1	0.365	0.928	2.09	26.5
Spatial model 2	0.348	0.928	2.02	42.7

Table 4: Predictive performance of different approaches for the NOAA monthly gridded temperature dataset. The standard deviation of the outcomes in this dataset is 0.940. The results of the FRK, GOLF and LAGP are given in the first to third rows. For the results in the fourth and fifth rows, we fit both spatial models of using the **RobustGaSP** package with one initial value and two initial values of the range and nugget parameters for finding the marginal posterior mode, respectively.

data from Jan, 1999 to Dec, 2018. For each month, we observe the temperature anomalies at  $n_1 = 36 \times 28$  spatial grids with longitude ranging from 182.5 to 357.5, and with latitude ranging from -62.5 to 72.5, respectively. There are 11,122 missing data, leaving the total number of observations to be 230,798. We held out 50% randomly sampled temperature anomalies as the missing data and the rest 50% is used as training data (i.e.  $n = n^* = 115,399$ ). Predicting the missing values in this scenario is more difficult than the example in (Gu and Shen, 2020), where the data are missing in a set of locations over the same months.

We fit the GOLF processes on the training data set, where the separable Matérn covariance is used for the two spatial coordinates, and the factors processes are defined on the temporal input. We assume different kernel parameters of the factor processes, which leads to a nonseparable spatio-temporal covariance function. Due to computational limitation, we let the number of factors be  $d = 0.75^2 n_1 = 567$  by letting the factor loadings to be a kronecker product of the first three quarters of the eigenvectors of the sub-covariance matrices for longitude and latitude. Although we have a large number of factors, the computational operations are  $O(Nd_{max})$  with  $d_{max} = 0.75 \times 36 = 48$  rather than  $O(Nd_1d_2)$  by the mode multiplication of tensor (see Section 3.3 for the discussion). We assume the coefficients of the intercept and linear coefficients are different at each location, i.e.  $\mathbf{M} = (\mathbf{H}_2\mathbf{B}_2)^T$  where  $\mathbf{H}_2 = [\mathbf{1}_{n_2}, \mathbf{x}]$ , with  $\mathbf{x}$  being 240 months and  $\mathbf{B}_2$  being a  $2 \times n_1$  coefficients. We use  $M = 3000$  MCMC samples with the first 20% as the burn-in samples. We only need a small posterior sample size for this example as the prediction converges fast when the data are missing at random.

In Table 4, we compare the GOLF processes with a few other spatial and spatio-temporal methods for the NOAA dataset. We fit two spatial models separately for each month using the **RobustGaSP** package with one or two sets of initial values in finding the marginal posterior mode of the kernel parameters (Gu et al., 2019). We also implemented the fixed rank Kriging (FRK) and local Gaussian process approximation (LAGP) by the **FRK** and **laGP** packages (Zammit-Mangion and Cressie, 2017; Gramacy, 2016), respectively.

As shown in Table 4, the GOLF processes have the smallest predictive RMSE and shortest predictive interval that covers around 94% of the held-out output. Since the temporal input is not used, it is not surprising that the RMSE and the length of predictive interval of the two

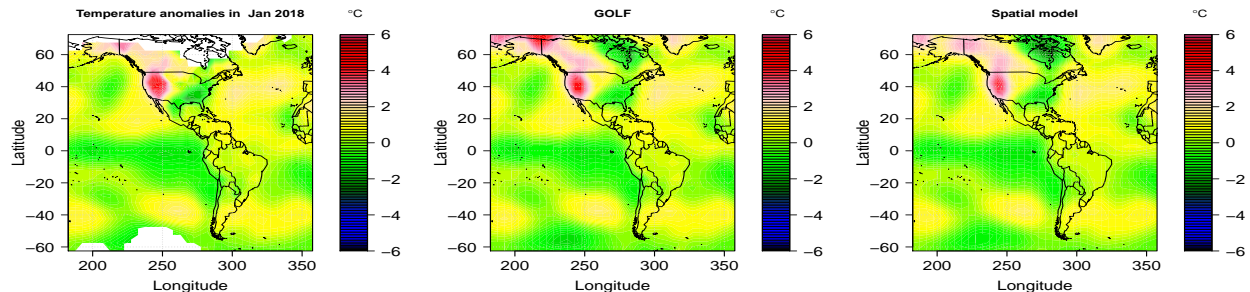


Figure 6: Full temperature, prediction from GOLF and spatial model by RobustGaSP package with two initial values.

spatial models are larger than the ones by the GOLF processes. If we include the temporal inputs, the computation cost is too large for directly inverting the covariance matrix. The FRK and LAGP also seem to have a larger predictive error, though both the spatial and temporal inputs are used in these methods.

The GOLF processes seem to be more accurate due to three reasons. First, the range parameters in orthogonal factor loadings and kernel functions of factor processes are estimated based on the posterior distribution. Because of orthogonal decomposition of the likelihood and posterior independence of factor processes, no approximation is needed to compute the likelihood function for this large data set. Second, the mean and trend parameters at each location in the GOLF processes are different, making the model flexible to estimate the trend of increasing temperature values over time. Finally, note that we integrate out the factor processes to sample the parameters from the marginal posterior distribution, and in addition, the mean parameters are also marginalized out when sample the kernel parameters and variance parameters. The marginalization step is important to alleviate the identifiability issue.

In Figure 6, we graph the full temperature anomalies in Jan 2018, predictions from the GOLF and spatial GP model by RobustGaSP package. 50% of the observation in the left panel are held out for testing. Both models seem to be accurate. Since the temporal coordinate is used in prediction, the predictive error by GOLF processes is smaller.

## 7 Concluding remarks

We have introduced the GOLF processes, as a computationally feasible approach for large correlated data. The orthogonal decomposition of the likelihood function and posterior independence of the factor processes allow one to reduce the computational burden in computing the inversion and the determinant of the covariance matrix in a Gaussian process. We have also discussed a flexible way to model the mean function when the sample size is large, and have derived the closed-form marginal likelihood to alleviate the identifiability issue. The proposed MCMC algorithm and continuous-time Kalman filter allow us to apply full Bayesian inference on large incomplete matrices of spatial, spatio-temporal and function data.

The computational tools developed in this work require observations from a matrix or



array with potential missing values. Future extensions of model for data with other input designs will be useful. Second, a principle way to select the number of factors and a study of asymptotic behaviors are important to develop an algorithm with default choice of prior parameters. Furthermore, we assume the errors follow a Gaussian distributions with the same variance parameters in this work, and the extension of this model for observations with heterogeneous noises will be helpful for some applications. Finally, we derive the full Bayesian analysis in this work. Constructing an expectation-maximization algorithm may be useful to reduce the number of posterior samples.

## Supplementary material

Supplement to “Gaussian orthogonal latent factor processes for large incomplete matrices of correlated data”. The supplementary material consists of three parts: the proofs for Section 2, the additional results of the simulated studies and the real applications.

## References

- Anderson, K. R., Johanson, I. A., Patrick, M. R., Gu, M., Segall, P., Poland, M. P., Montgomery-Brown, E. K., and Miklius, A. (2019). Magma reservoir failure and the onset of caldera collapse at kilauea volcano in 2018. *Science*, 366(6470).
- Bai, Z., Demmel, J., Dongarra, J., Ruhe, A., and Vorst, H. v. d. (2000). *Templates for the solution of algebraic eigenvalue problems: a practical guide*. Society for Industrial and Applied Mathematics.
- Banerjee, S., Carlin, B. P., and Gelfand, A. E. (2014). *Hierarchical modeling and analysis for spatial data*. CRC Press.
- Banerjee, S., Gelfand, A. E., Finley, A. O., and Sang, H. (2008). Gaussian predictive process models for large spatial data sets. *Journal of the Royal Statistical Society: Series B (Statistical Methodology)*, 70(4):825–848.
- Bayarri, M. J., Berger, J. O., Calder, E. S., Dalbey, K., Lunagomez, S., Patra, A. K., Pitman, E. B., Spiller, E. T., and Wolpert, R. L. (2009). Using statistical and computer models to quantify volcanic hazards. *Technometrics*, 51:402–413.
- Conti, S. and O’Hagan, A. (2010). Bayesian emulation of complex multi-output and dynamic computer models. *Journal of statistical planning and inference*, 140(3):640–651.
- Cressie, N. and Johannesson, G. (2008). Fixed rank kriging for very large spatial data sets. *Journal of the Royal Statistical Society: Series B (Statistical Methodology)*, 70(1):209–226.
- Cressie, N. A. and Cassie, N. A. (1993). *Statistics for spatial data*. Wiley, New York.
- Datta, A., Banerjee, S., Finley, A. O., and Gelfand, A. E. (2016). Hierarchical nearest-neighbor gaussian process models for large geostatistical datasets. *Journal of the American Statistical Association*, 111(514):800–812.



- Gelfand, A. E., Diggle, P., Guttorp, P., and Fuentes, M. (2010). *Handbook of spatial statistics*. CRC Press.
- Gelfand, A. E., Schmidt, A. M., Banerjee, S., and Sirmans, C. (2004). Nonstationary multivariate process modeling through spatially varying coregionalization. *Test*, 13(2):263–312.
- Gramacy, R. B. (2016). lagp: large-scale spatial modeling via local approximate gaussian processes in r. *Journal of Statistical Software*, 72(1):1–46.
- Gramacy, R. B. and Apley, D. W. (2015). Local Gaussian process approximation for large computer experiments. *Journal of Computational and Graphical Statistics*, 24(2):561–578.
- Gu, M. (2018). Jointly robust prior for Gaussian stochastic process in emulation, calibration and variable selection. *Bayesian Analysis*, 14(1).
- Gu, M., Palomo, J., and Berger, J. O. (2019). RobustGaSP: Robust Gaussian Stochastic Process Emulation in R. *The R Journal*, 11(1):112–136.
- Gu, M. and Shen, W. (2020). Generalized probabilistic principal component analysis of correlated data. *Journal of Machine Learning Research*, 21(13).
- Gu, M. and Xu, Y. (2020). Fast nonseparable Gaussian stochastic process with application to methylation level interpolation. *Journal of Computational and Graphical Statistics*, 29(2):250–260.
- Guinness, J. and Fuentes, M. (2017). Circulant embedding of approximate covariances for inference from gaussian data on large lattices. *Journal of computational and Graphical Statistics*, 26(1):88–97.
- Hartikainen, J. and Sarkka, S. (2010). Kalman filtering and smoothing solutions to temporal gaussian process regression models. In *Machine Learning for Signal Processing (MLSP), 2010 IEEE International Workshop on*, pages 379–384. IEEE.
- Heaton, M. J., Datta, A., Finley, A. O., Furrer, R., Guinness, J., Guhaniyogi, R., Gerber, F., Gramacy, R. B., Hammerling, D., Katzfuss, M., et al. (2019). A case study competition among methods for analyzing large spatial data. *Journal of Agricultural, Biological and Environmental Statistics*, 24(3):398–425.
- Higdon, D., Gattiker, J., Williams, B., and Rightley, M. (2008). Computer model calibration using high-dimensional output. *Journal of the American Statistical Association*, 103(482):570–583.
- Katzfuss, M. (2017). A multi-resolution approximation for massive spatial datasets. *Journal of the American Statistical Association*, 112(517):201–214.
- Katzfuss, M. and Guinness, J. (2017). A general framework for vecchia approximations of gaussian processes. *arXiv preprint arXiv:1708.06302*.

- Kaufman, C. G., Schervish, M. J., and Nychka, D. W. (2008). Covariance tapering for likelihood-based estimation in large spatial data sets. *Journal of the American Statistical Association*, 103(484):1545–1555.
- Kennedy, M. C. and O’Hagan, A. (2001). Bayesian calibration of computer models. *Journal of the Royal Statistical Society: Series B (Statistical Methodology)*, 63(3):425–464.
- Kolda, T. G. and Bader, B. W. (2009). Tensor decompositions and applications. *SIAM review*, 51(3):455–500.
- Lindgren, F., Rue, H., and Lindström, J. (2011). An explicit link between gaussian fields and gaussian markov random fields: the stochastic partial differential equation approach. *Journal of the Royal Statistical Society: Series B (Statistical Methodology)*, 73(4):423–498.
- Paulo, R. (2005). Default priors for Gaussian processes. *Annals of statistics*, 33(2):556–582.
- Paulo, R., García-Donato, G., and Palomo, J. (2012). Calibration of computer models with multivariate output. *Computational Statistics and Data Analysis*, 56(12):3959–3974.
- Petris, G., Petrone, S., and Campagnoli, P. (2009). *Dynamic linear models with R*. Springer.
- Prado, R. and West, M. (2010). *Time series: modeling, computation, and inference*. CRC Press.
- Rasmussen, C. E. (2006). *Gaussian processes for machine learning*. MIT Press.
- Rue, H., Martino, S., and Chopin, N. (2009). Approximate bayesian inference for latent gaussian models by using integrated nested laplace approximations. *Journal of the royal statistical society: Series B (statistical methodology)*, 71(2):319–392.
- Sacks, J., Welch, W. J., Mitchell, T. J., Wynn, H. P., et al. (1989). Design and analysis of computer experiments. *Statistical science*, 4(4):409–423.
- Sang, H. and Huang, J. Z. (2012). A full scale approximation of covariance functions for large spatial data sets. *Journal of the Royal Statistical Society: Series B (Statistical Methodology)*, 74(1):111–132.
- Särkkä, S. and Hartikainen, J. (2012). Infinite-dimensional kalman filtering approach to spatio-temporal gaussian process regression. In *International Conference on Artificial Intelligence and Statistics*, pages 993–1001.
- Seeger, M., Teh, Y.-W., and Jordan, M. (2005). Semiparametric latent factor models. Technical report.
- Stein, M. L. (2014). Limitations on low rank approximations for covariance matrices of spatial data. *Spatial Statistics*, 8:1–19.
- Stroud, J. R., Stein, M. L., and Lysen, S. (2017). Bayesian and maximum likelihood estimation for gaussian processes on an incomplete lattice. *Journal of computational and Graphical Statistics*, 26(1):108–120.

- Vecchia, A. V. (1988). Estimation and model identification for continuous spatial processes. *Journal of the Royal Statistical Society: Series B (Methodological)*, 50(2):297–312.
- West, M. and Harrison, P. J. (1997). *Bayesian Forecasting & Dynamic Models*. Springer Verlag, 2nd edition.
- Whittle, P. (1954). On stationary processes in the plane. *Biometrika*, pages 434–449.
- Whittle, P. (1963). Stochastic process in several dimensions. *Bulletin of the International Statistical Institute*, 40(2):974–994.
- Zammit-Mangion, A. and Cressie, N. (2017). Frk: An r package for spatial and spatio-temporal prediction with large datasets. *arXiv preprint arXiv:1106.6251*.
- Zimmerman, D. L. (1993). Another look at anisotropy in geostatistics. *Mathematical Geology*, 25(4):453–470.

# Supplementary materials: Gaussian orthogonal latent factor processes for large incomplete matrices of correlated data

This supplementary materials contain three parts. The proof of Section 2 is given in Section S1. The additional numerical results for the simulated studies and real applications are given in Section S2 and Section S3, respectively.

## S1 Proofs for Section 2

### S1.1 Auxiliary facts

1. Let  $\mathbf{A}$  and  $\mathbf{B}$  be matrices,

$$(\mathbf{A} \otimes \mathbf{B})^T = (\mathbf{A}^T \otimes \mathbf{B}^T);$$

further assuming  $\mathbf{A}$  and  $\mathbf{B}$  are invertible,

$$(\mathbf{A} \otimes \mathbf{B})^{-1} = \mathbf{A}^{-1} \otimes \mathbf{B}^{-1}.$$

2. Let  $\mathbf{A}$ ,  $\mathbf{B}$ ,  $\mathbf{C}$  and  $\mathbf{D}$  be the matrices such that the products  $\mathbf{AC}$  and  $\mathbf{BD}$  are matrices,

$$(\mathbf{A} \otimes \mathbf{B})(\mathbf{C} \otimes \mathbf{D}) = (\mathbf{AC}) \otimes (\mathbf{BD}).$$

3. For matrices  $\mathbf{A}$ ,  $\mathbf{B}$  and  $\mathbf{C}$ ,

$$(\mathbf{C}^T \otimes \mathbf{A})\text{vec}(\mathbf{B}) = \text{vec}(\mathbf{ABC});$$

further assuming  $\mathbf{A}^T\mathbf{B}$  is a matrix,

$$\text{tr}(\mathbf{A}^T\mathbf{B}) = \text{vec}(\mathbf{A})^T\text{vec}(\mathbf{B}).$$

4. For any invertible  $n \times n$  matrix  $\mathbf{C}$ ,

$$|\mathbf{C} + \mathbf{AB}| = |\mathbf{C}||\mathbf{I}_n + \mathbf{BC}^{-1}\mathbf{A}|.$$

### S1.2 Proofs for Section 2.1

The following denotation are used in the proof:  $\mathbf{Y}_{-M} = \mathbf{Y} - \mathbf{M}$ ,  $\mathbf{Y}_{v,-M} = \text{vec}(\mathbf{Y} - \mathbf{M})$ ,  $\mathbf{Z}_{vt} = \text{vec}(\mathbf{Z}^T)$  and  $\mathbf{A}_v = [\mathbf{I}_n \otimes \mathbf{a}_1, \dots, \mathbf{I}_n \otimes \mathbf{a}_d]$ . Let  $\Sigma_v$  be an  $nd \times nd$  matrix where the  $l$ th diagonal block is  $\Sigma_l$ . Denote  $\text{etr}(\cdot) = \exp(\text{tr}(\cdot))$ .

*Proof of Equation 4.* Denote  $C_Y = (2\pi\sigma_0^2)^{-\frac{nk}{2}} \prod_{l=1}^d |\Sigma_l/\sigma_0^2 + \mathbf{I}_k|^{-1/2}$ . Directly marginalizing out  $\mathbf{Z}$ , one has

$$\begin{aligned}
& p(\mathbf{Y} \mid \Theta) \\
&= C_Y \exp \left( -\frac{\mathbf{Y}_{v,-M}^T \left( \mathbf{I}_{nk} - \sum_{l=1}^d (\sigma_0^2 \Sigma_l^{-1} + \mathbf{I}_n)^{-1} \otimes (\mathbf{a}_l \mathbf{a}_l^T) \right) \mathbf{Y}_{v,-M}}{2\sigma_0^2} \right) \\
&= C_Y \exp \left( -\frac{\mathbf{Y}_{v,-M}^T \mathbf{Y}_{v,-M} - \mathbf{Y}_{v,-M}^T \sum_{l=1}^d \text{vec}(\mathbf{a}_l \mathbf{a}_l^T \mathbf{Y}_{v,-M} (\sigma_0^2 \Sigma_l^{-1} + \mathbf{I}_n)^{-1})}{2\sigma_0^2} \right) \\
&= C_Y \text{etr} \left( -\frac{\mathbf{Y}_{-M}^T \mathbf{Y}_{-M} - \sum_{l=1}^d \tilde{\mathbf{y}}_l \tilde{\mathbf{y}}_l^T (\sigma_0^2 \Sigma_l^{-1} + \mathbf{I}_n)^{-1}}{2\sigma_0^2} \right) \\
&= C_Y \exp \left( -\frac{\sum_{l=1}^d \tilde{\mathbf{y}}_l^T (\Sigma_l/\sigma_0^2 + \mathbf{I}_n)^{-1} \tilde{\mathbf{y}}_l + \sum_{l=d+1}^{n_1} \tilde{\mathbf{y}}_l^T \tilde{\mathbf{y}}_l}{2\sigma_0^2} \right),
\end{aligned}$$

where the first equation is based on Lemma 1 and the Woodbury matrix identity (to compute the normalizing constant  $C_Y$ ); the second and third equations are from fact 3; the fourth equation is from Woodbury matrix identity. The Equation (4) follows immediately.  $\square$

*Proof of Corollary 1.* The proof is implied by the proof of Theorem 4 in (Gu and Shen, 2020). For completeness of this article, we include the proof below.

From Equation (1) and Equation (2), we have

$$\begin{aligned}
p(\mathbf{Z}_{vt} \mid \mathbf{Y}, \Theta) &\propto \exp \left( \frac{(\mathbf{Y}_{v,-M} - \mathbf{A}_v \mathbf{Z}_{vt})^T (\mathbf{Y}_{v,-M} - \mathbf{A}_v \mathbf{Z}_{vt})}{2\sigma_0^2} \right) \exp \left( -\frac{1}{2} \mathbf{Z}_{vt}^T \Sigma_v^{-1} \mathbf{Z}_{vt} \right) \\
&\propto \exp \left\{ -\frac{1}{2} (\mathbf{Z}_{vt} - \boldsymbol{\mu}_{Z_{vt}})^T \left( \frac{\mathbf{A}_v^T \mathbf{A}_v}{\sigma_0^2} + \Sigma_v^{-1} \right) (\mathbf{Z}_{vt} - \boldsymbol{\mu}_{Z_{vt}}) \right\},
\end{aligned}$$

where  $\boldsymbol{\mu}_{Z_{vt}} = (\mathbf{A}_v^T \mathbf{A}_v + \sigma_0^2 \Sigma_v^{-1})^{-1} \mathbf{A}_v^T \mathbf{Y}_{v,-M}$ . Note  $\mathbf{A}_v^T \mathbf{A}_v = \mathbf{I}_{nd}$ , from which we have

$$\mathbf{Z}_{vt} \mid \mathbf{Y}, \Theta \sim \text{MN} \left( \boldsymbol{\mu}_{Z_{vt}}, \left( \frac{1}{\sigma_0^2} \mathbf{I}_{n_1 n_2} + \Sigma_v^{-1} \right)^{-1} \right). \quad (\text{S1})$$

Based on vectorization, one has

$$\begin{aligned}
\boldsymbol{\mu}_{Z_{vt}} &= \begin{pmatrix} (\sigma_0^2 \Sigma_1^{-1} + \mathbf{I}_n)^{-1} \otimes \mathbf{a}_1^T \\ \vdots \\ (\sigma_0^2 \Sigma_d^{-1} + \mathbf{I}_n)^{-1} \otimes \mathbf{a}_d^T \end{pmatrix} \text{vec}(\mathbf{Y}) = \begin{pmatrix} \text{vec} \left( \mathbf{a}_1^T \mathbf{Y}_{-M} (\sigma_0^2 \Sigma_1^{-1} + \mathbf{I}_n)^{-1} \right) \\ \vdots \\ \text{vec} \left( \mathbf{a}_d^T \mathbf{Y}_{-M} (\sigma_0^2 \Sigma_d^{-1} + \mathbf{I}_n)^{-1} \right) \end{pmatrix} \\
&= \text{vec} \left( \begin{pmatrix} \mathbf{a}_1^T \mathbf{Y}_{-M} (\sigma_0^2 \Sigma_1^{-1} + \mathbf{I}_n)^{-1} \\ \vdots \\ \mathbf{a}_d^T \mathbf{Y}_{-M} (\sigma_0^2 \Sigma_d^{-1} + \mathbf{I}_n)^{-1} \end{pmatrix}^T \right). \quad (\text{S2})
\end{aligned}$$

Note that the covariance matrix of  $\boldsymbol{\mu}_{Z_{vt}}$  is a block diagonal matrix. The results follow by Equation (S2) and the Woodbury matrix identity.  $\square$

### S1.3 Proofs for Section 2.2

Note  $\mathbf{A}_F = [\mathbf{A}_s, \mathbf{A}_c] = [\mathbf{a}_1, \mathbf{a}_2, \dots, \mathbf{a}_{n_1}]$ , where  $\mathbf{A}_c$  is an  $n_1 \times (n_1 - d)$  matrix of the orthogonal complement of  $\mathbf{A}_s$ . We need the following lemma to prove Theorem 1.

**Lemma S1.** *After marginalizing out the factors  $\mathbf{Z}$ , we have the marginal posterior distribution of the transformed regression coefficients,*

1. *(Marginal distribution of transformed row regression coefficients). Assume  $\mathbf{M} = \mathbf{H}_1 \mathbf{B}_1$  and the objective prior  $\pi(\mathbf{B}_1) \propto 1$  for  $\mathbf{B}_1$ . Let  $\tilde{\mathbf{B}}_1 = [\tilde{\mathbf{b}}_{1,1}, \dots, \tilde{\mathbf{b}}_{1,n_1}] = \mathbf{B}_1^T \mathbf{H}_1^T \mathbf{A}_F$  be an  $n_2 \times n_1$  matrix of transformed coefficients. Assume the marginal posterior distribution of  $\tilde{\mathbf{B}}_1$  follows*

$$p(\tilde{\mathbf{B}}_1 \mid \mathbf{Y}, \boldsymbol{\Theta}_{-B_1}) = \prod_{l=1}^d \mathcal{PN}(\tilde{\mathbf{b}}_{1,l}; \tilde{\mathbf{y}}_l, \tilde{\boldsymbol{\Sigma}}_l) \prod_{l=d+1}^{n_1} \mathcal{PN}(\tilde{\mathbf{b}}_{1,l}; \tilde{\mathbf{y}}_l, \sigma_0^2 \mathbf{I}_{n_2}), \quad (\text{S3})$$

where  $\tilde{\mathbf{y}}_l$  is defined in equation (4) and  $\tilde{\boldsymbol{\Sigma}}_l$  is defined in corollary 1. Then we can sample  $(\mathbf{B}_1 \mid \mathbf{Y}, \boldsymbol{\Theta}_{-B_1})$  by  $(\mathbf{H}_1^T \mathbf{H}_1)^{-1} \mathbf{H}_1^T \mathbf{A}_F \tilde{\mathbf{B}}_1^T$ , where  $\tilde{\mathbf{B}}_1^T$  are sampled from the  $p(\tilde{\mathbf{B}}_1 \mid \mathbf{Y}, \boldsymbol{\Theta}_{-B_1})$  in equation (S3).

2. *(Marginal distribution of transformed column regression coefficients). Assume  $\mathbf{M} = (\mathbf{H}_2 \mathbf{B}_2)^T$  and the objective prior  $\pi(\mathbf{B}_2) \propto 1$  for the regression parameters  $\mathbf{B}_2$ . Let  $\tilde{\mathbf{B}}_2 = [\tilde{\mathbf{b}}_{2,1}, \dots, \tilde{\mathbf{b}}_{2,n_1}] = \mathbf{B}_2 \mathbf{A}_F$  be a  $q_2 \times n_1$  matrix. The marginal posterior distribution of  $\tilde{\mathbf{B}}_2$  follows*

$$p(\tilde{\mathbf{B}}_2 \mid \mathbf{Y}, \boldsymbol{\Theta}_{-B_2}) = \prod_{l=1}^{n_1} \mathcal{PN}(\tilde{\mathbf{b}}_{2,l}; \boldsymbol{\mu}_{\tilde{\mathbf{b}}_{2,l}}, \boldsymbol{\Sigma}_{\tilde{\mathbf{b}}_{2,l}}), \quad (\text{S4})$$

where  $\boldsymbol{\mu}_{\tilde{\mathbf{b}}_{2,l}} = (\mathbf{H}_2^T \tilde{\boldsymbol{\Sigma}}_l^{-1} \mathbf{H}_2)^{-1} \mathbf{H}_2^T \tilde{\boldsymbol{\Sigma}}_l^{-1} \tilde{\mathbf{y}}_l$  and  $\boldsymbol{\Sigma}_{\tilde{\mathbf{b}}_{2,l}} = (\mathbf{H}_2^T \tilde{\boldsymbol{\Sigma}}_l^{-1} \mathbf{H}_2)^{-1}$  for  $l = 1, \dots, d$ ;  $\boldsymbol{\mu}_{\tilde{\mathbf{b}}_{2,l}} = (\mathbf{H}_2^T \mathbf{H}_2)^{-1} \mathbf{H}_2^T \tilde{\mathbf{y}}_l$  and  $\boldsymbol{\Sigma}_{\tilde{\mathbf{b}}_{2,l}} = \sigma_0^2 (\mathbf{H}_2^T \mathbf{H}_2)^{-1}$  for  $l = d+1, \dots, n_1$ .

*Proof of Lemma S1.* 1. (Marginal distribution of transformed row regression coefficients).

Denote  $(\mathbf{B}_1^{aug}) = [\mathbf{B}_1^T, \tilde{\mathbf{B}}_{1,(q_1+1):n_1}]^T$ , where  $\tilde{\mathbf{B}}_{1,(q_1+1):n_1}$  are the last  $n_1 - q_1$  columns of  $\tilde{\mathbf{B}}_1$ . Denote  $p_{trans}(\mathbf{B}_1 \mid \mathbf{Y}, \boldsymbol{\Theta}_{-B_1})$  and  $p_{trans}(\mathbf{B}_1^{aug} \mid \mathbf{Y}, \boldsymbol{\Theta}_{-B_1})$  the transformed marginal posterior distribution of  $\mathbf{B}_1$  and  $\mathbf{B}_1^{aug}$  derived by transforming  $p(\tilde{\mathbf{B}}_1 \mid \mathbf{Y}, \boldsymbol{\Theta}_{-B_1})$  in (S3).

We have

$$\begin{aligned}
p_{trans}(\mathbf{B}_1 \mid \mathbf{Y}, \boldsymbol{\Theta}_{-\mathbf{B}_1}) &\propto p_{trans}(\mathbf{B}_1^{aug} \mid \mathbf{Y}, \boldsymbol{\Theta}_{-\mathbf{B}_1}) = p(\tilde{\mathbf{B}}_1 \mid \mathbf{Y}, \boldsymbol{\Theta}_{-\mathbf{B}_1}) \left| \frac{d\tilde{\mathbf{B}}_1}{d\mathbf{B}_1^{aug}} \right| \\
&\propto \exp \left\{ -\frac{1}{2} \sum_{l=1}^d (\tilde{\mathbf{b}}_{1,l} - \tilde{\mathbf{y}}_l)^T \tilde{\boldsymbol{\Sigma}}_l^{-1} (\tilde{\mathbf{b}}_{1,l} - \tilde{\mathbf{y}}_l) - \frac{1}{2\sigma_0^2} \sum_{l=d+1}^{n_1} (\tilde{\mathbf{b}}_{1,l} - \tilde{\mathbf{y}}_l)^T (\tilde{\mathbf{b}}_{1,l} - \tilde{\mathbf{y}}_l) \right\} \\
&\propto \exp \left\{ -\frac{1}{2} \sum_{l=1}^d \mathbf{a}_l^T (\mathbf{Y} - \mathbf{H}_1 \mathbf{B}_1) \tilde{\boldsymbol{\Sigma}}_l^{-1} (\mathbf{Y} - \mathbf{H}_1 \mathbf{B}_1)^T \mathbf{a}_l \right. \\
&\quad \left. - \frac{1}{2\sigma_0^2} \sum_{l=d+1}^{n_1} \mathbf{a}_l^T (\mathbf{Y} - \mathbf{H}_1 \mathbf{B}_1) (\mathbf{Y} - \mathbf{H}_1 \mathbf{B}_1)^T \mathbf{a}_l \right\},
\end{aligned}$$

where the last line is the same as the posterior distribution of  $\mathbf{B}_1$  based on the marginal likelihood in equation (4) and the prior distribution  $\pi(\mathbf{B}_1) \propto 1$ . Thus if one sample  $\tilde{\mathbf{B}}_1$  from (S3), one can obtain the sample for  $(\mathbf{B}_1 \mid \mathbf{Y}, \boldsymbol{\Theta}_{-\mathbf{B}_1})$  through  $(\mathbf{H}_1^T \mathbf{H}_1)^{-1} \mathbf{H}_1^T \mathbf{A}_F \tilde{\mathbf{B}}_1^T$ .

2. (Marginal distribution of transformed column regression coefficients).

Since  $\pi(\mathbf{B}_2) \propto 1$  is a Jeffreys prior, and  $\tilde{\mathbf{B}}_2$  is a linear transformation of  $\mathbf{B}_2$  with the same dimension, we have  $\pi(\tilde{\mathbf{B}}_2) \propto 1$ .

Based on the marginal likelihood in equation (4) and the prior distribution, the posterior distribution of  $\tilde{\mathbf{B}}_2$  follows:

$$\begin{aligned}
&p(\tilde{\mathbf{B}}_2 \mid \mathbf{Y}, \boldsymbol{\Theta}_{-\mathbf{B}_2}) \\
&\propto \exp \left\{ -\frac{1}{2} \sum_{l=1}^d \mathbf{a}_l^T (\mathbf{Y} - \mathbf{B}_2^T \mathbf{H}_2^T) \tilde{\boldsymbol{\Sigma}}_l^{-1} (\mathbf{Y} - \mathbf{B}_2^T \mathbf{H}_2^T)^T \mathbf{a}_l \right. \\
&\quad \left. - \frac{1}{2\sigma_0^2} \sum_{l=d+1}^{n_1} \mathbf{a}_l^T (\mathbf{Y} - \mathbf{B}_2^T \mathbf{H}_2^T) (\mathbf{Y} - \mathbf{B}_2^T \mathbf{H}_2^T)^T \mathbf{a}_l \right\} \\
&\propto \exp \left\{ -\frac{1}{2} \sum_{l=1}^d (\tilde{\mathbf{y}}_l - \mathbf{H}_2 \tilde{\mathbf{b}}_{2,l})^T \tilde{\boldsymbol{\Sigma}}_l^{-1} (\tilde{\mathbf{y}}_l - \mathbf{H}_2 \tilde{\mathbf{b}}_{2,l}) \right. \\
&\quad \left. - \frac{1}{2\sigma_0^2} \sum_{l=d+1}^{n_1} (\tilde{\mathbf{y}}_l - \mathbf{H}_2 \tilde{\mathbf{b}}_{2,l})^T (\tilde{\mathbf{y}}_l - \mathbf{H}_2 \tilde{\mathbf{b}}_{2,l}) \right\} \\
&\propto \exp \left\{ -\frac{1}{2} \sum_{l=1}^d \left( \tilde{\mathbf{b}}_{2,l} - \boldsymbol{\mu}_{\tilde{\mathbf{b}}_{2,l}} \right)^T \mathbf{H}_2^T \tilde{\boldsymbol{\Sigma}}_l^{-1} \mathbf{H}_2 \left( \tilde{\mathbf{b}}_{2,l} - \boldsymbol{\mu}_{\tilde{\mathbf{b}}_{2,l}} \right) \right. \\
&\quad \left. - \frac{1}{2\sigma_0^2} \sum_{l=d+1}^{n_1} \left( \tilde{\mathbf{b}}_{2,l} - \boldsymbol{\mu}_{\tilde{\mathbf{b}}_{2,l}} \right)^T \mathbf{H}_2^T \mathbf{H}_2 \left( \tilde{\mathbf{b}}_{2,l} - \boldsymbol{\mu}_{\tilde{\mathbf{b}}_{2,l}} \right) \right\},
\end{aligned}$$

from which equation (S4) follows. □

We are ready to prove Theorem 1.

*Proof of Theorem 1.* After marginalizing out  $\mathbf{Z}$ , we have

1. (Row regression coefficients).

From Lemma S1, the posterior mean of  $(\tilde{\mathbf{B}}_1 \mid \mathbf{Y}, \boldsymbol{\Theta}_{-\mathbf{B}_1})$  is  $\mathbf{Y}^T \mathbf{A}_F$ , where  $\mathbf{A}_F := [\mathbf{A}_s, \mathbf{A}_c]$ . We denote the centered  $\tilde{\mathbf{B}}_1$  by  $\tilde{\mathbf{B}}_{1,0} = [\tilde{\mathbf{B}}_{1,0,s}, \tilde{\mathbf{B}}_{1,0,c}] = \tilde{\mathbf{B}}_1 - \mathbf{Y}^T \mathbf{A}_F$ , where  $\tilde{\mathbf{B}}_{1,0,s}$  is the first  $d$  columns of  $\tilde{\mathbf{B}}_{1,0}$  and  $\tilde{\mathbf{B}}_{1,0,c}$  is the last  $(n_1 - d)$  columns of  $\tilde{\mathbf{B}}_{1,0}$ . Let  $\tilde{\mathbf{b}}_{1,0,l}$  be the  $l$ -th column of  $\tilde{\mathbf{B}}_{1,0}$ . Then the posterior mean of  $(\mathbf{B}_1 \mid \mathbf{Y}, \boldsymbol{\Theta}_{-\mathbf{B}_1})$  can be calculated below

$$\begin{aligned} \hat{\mathbf{B}}_1 &= \mathbb{E}(\mathbf{B}_1 \mid \mathbf{Y}, \boldsymbol{\Theta}_{-\mathbf{B}_1}) = \mathbb{E} \left( (\mathbf{H}_1^T \mathbf{H}_1)^{-1} \mathbf{H}_1^T \mathbf{A}_F \tilde{\mathbf{B}}_1^T \mid \mathbf{Y}, \boldsymbol{\Theta}_{-\mathbf{B}_1} \right) \\ &= (\mathbf{H}_1^T \mathbf{H}_1)^{-1} \mathbf{H}_1^T \mathbf{A}_F \mathbf{A}_F^T \mathbf{Y} = (\mathbf{H}_1^T \mathbf{H}_1)^{-1} \mathbf{H}_1^T \mathbf{Y} \end{aligned}$$

Note  $\mathbf{B}_1 = (\mathbf{H}_1^T \mathbf{H}_1)^{-1} \mathbf{H}_1^T \mathbf{A}_F \tilde{\mathbf{B}}_1^T$ , one has

$$\mathbf{B}_1 - \hat{\mathbf{B}}_1 = (\mathbf{H}_1^T \mathbf{H}_1)^{-1} \mathbf{H}_1^T \mathbf{A}_F (\tilde{\mathbf{B}}_{1,0})^T = (\mathbf{H}_1^T \mathbf{H}_1)^{-1} \mathbf{H}_1^T \left( \mathbf{A}_s \tilde{\mathbf{B}}_{1,0,s}^T + \mathbf{A}_c \tilde{\mathbf{B}}_{1,0,c}^T \right)$$

where  $\tilde{\mathbf{B}}_{1,0,s}$  is a  $n_2 \times d$  matrix with the  $l$ th column independently sampled from  $\mathcal{N}(\mathbf{0}, \tilde{\boldsymbol{\Sigma}}_l)$  for  $l = 1, \dots, d$ . For the distribution of  $\mathbf{A}_c \tilde{\mathbf{B}}_{1,0,c}^T$ , using part 1 of Lemma S1, we have

$$\begin{aligned} p(\mathbf{A}_c \tilde{\mathbf{B}}_{1,0,c}^T \mid \mathbf{Y}, \boldsymbol{\Theta}_{-\mathbf{B}_1}) &\propto \exp \left\{ -\frac{1}{2\sigma_0^2} \text{tr} \left( \mathbf{A}_c^T \tilde{\mathbf{B}}_{1,0,c} \tilde{\mathbf{B}}_{1,0,c}^T \mathbf{A}_c \right) \right\} \\ &\propto \exp \left\{ -\frac{1}{2\sigma_0^2} \text{tr} \left( (\mathbf{I} - \mathbf{A}_s \mathbf{A}_s^T) \tilde{\mathbf{B}}_{1,0,c} \tilde{\mathbf{B}}_{1,0,c}^T \right) \right\}. \end{aligned}$$

Thus we can sample  $\mathbf{A}_c \tilde{\mathbf{B}}_{1,0,c}^T$  by  $\sigma_0(\mathbf{I} - \mathbf{A}_s \mathbf{A}_s^T) \mathbf{Z}_{0,1}$ , where  $\mathbf{Z}_{0,1}$  is an  $n_1 \times n_2$  matrix with each entry independently sampled from standard normal distribution. The results soon follow.

2. (Column regression coefficients).

We first compute the posterior mean of  $(\mathbf{B}_2 \mid \mathbf{Y}, \boldsymbol{\Theta}_{-\mathbf{B}_2})$  below

$$\begin{aligned} \hat{\mathbf{B}}_2 &= \mathbb{E}(\mathbf{B}_2 \mid \mathbf{Y}, \boldsymbol{\Theta}_{-\mathbf{B}_2}) = \mathbb{E}(\tilde{\mathbf{B}}_2 \mathbf{A}_F^T \mid \mathbf{Y}, \boldsymbol{\Theta}_{-\mathbf{B}_2}) \\ &= \sum_{l=1}^d (\mathbf{H}_2^T \tilde{\boldsymbol{\Sigma}}_l^{-1} \mathbf{H}_2)^{-1} \mathbf{H}_2^T \tilde{\boldsymbol{\Sigma}}_l^{-1} \mathbf{Y}^T \mathbf{a}_l \mathbf{a}_l^T + (\mathbf{H}_2^T \mathbf{H}_2)^{-1} \mathbf{H}_2^T \mathbf{Y}^T (\mathbf{I}_{n_1} - \mathbf{A}_s \mathbf{A}_s^T) \end{aligned}$$

We denote the centered  $\tilde{\mathbf{B}}_2$  by  $\tilde{\mathbf{B}}_{2,0} = [\tilde{\mathbf{B}}_{2,0,s}, \tilde{\mathbf{B}}_{2,0,c}]$ . We have

$$\mathbf{B}_2 - \hat{\mathbf{B}}_2 = \tilde{\mathbf{B}}_{2,0} \mathbf{A}_F^T = \tilde{\mathbf{B}}_{2,0,s} \mathbf{A}_s^T + \tilde{\mathbf{B}}_{2,0,c} \mathbf{A}_c^T$$



where  $\tilde{\mathbf{B}}_{2,0,s}$  is a  $q_2 \times d$  matrix with the  $l$ th column independently sampled from  $\mathcal{N}(\mathbf{0}, (\mathbf{H}_2^T \tilde{\Sigma}_l^{-1} \mathbf{H}_2)^{-1})$  for  $l = 1, \dots, d$ . For the distribution of  $\tilde{\mathbf{B}}_{2,0,c} \mathbf{A}_c^T$ , we have

$$\begin{aligned} p(\tilde{\mathbf{B}}_{2,0,c} \mathbf{A}_c^T \mid \mathbf{Y}, \boldsymbol{\Theta}_{-\mathbf{B}_2}) &\propto \exp \left\{ -\frac{1}{2\sigma_0^2} \text{tr} \left( \mathbf{A}_c \mathbf{A}_c^T \tilde{\mathbf{B}}_{2,0,c} \mathbf{H}_2^T \mathbf{H}_2 \tilde{\mathbf{B}}_{2,0,c}^T \right) \right\} \\ &\propto \exp \left\{ -\frac{1}{2\sigma_0^2} \text{tr} \left( (\mathbf{I} - \mathbf{A}_s \mathbf{A}_s^T) \tilde{\mathbf{B}}_{2,0,c} \mathbf{H}_2^T \mathbf{H}_2 \tilde{\mathbf{B}}_{2,0,c}^T \right) \right\}. \end{aligned}$$

Thus we can sample  $\tilde{\mathbf{B}}_{2,0,c} \mathbf{A}_c^T$  by  $\sigma_0(\mathbf{I}_{n_1} - \mathbf{A}_s \mathbf{A}_s^T) \mathbf{Z}_{0,2}^T \mathbf{L}_{H_2}^T$ , where  $\mathbf{L}_{H_2}$  is a  $q_2 \times q_2$  matrix such that  $\mathbf{L}_{H_2} \mathbf{L}_{H_2}^T = (\mathbf{H}_2^T \mathbf{H}_2)^{-1}$  and  $\mathbf{Z}_{0,2}$  is a  $q_2 \times n_1$  matrix with each entry independently sampled from standard normal distribution. □

**Lemma S2.** Assume  $\mathbf{M} = \mathbf{H}_1 \mathbf{B}_1 + (\mathbf{H}_2 \mathbf{B}_2)^T$  and let the objective prior  $\pi(\mathbf{B}_1, \mathbf{B}_2) \propto 1$  for the regression parameters  $\mathbf{B}_1$  and  $\mathbf{B}_2$ . Denote  $\tilde{\mathbf{B}}_1 = [\tilde{\mathbf{b}}_{1,1}, \dots, \tilde{\mathbf{b}}_{1,n_1}] = \mathbf{B}_1^T \mathbf{H}_1^T \mathbf{A}_F$  and  $\tilde{\mathbf{B}}_2 = [\tilde{\mathbf{b}}_{2,1}, \dots, \tilde{\mathbf{b}}_{2,n_1}] = \mathbf{B}_2 \mathbf{A}_F$ .

1. After marginalizing out  $\mathbf{Z}$  and  $\mathbf{B}_1$ , assume the marginal posterior distribution of  $\tilde{\mathbf{B}}_1$  follows

$$p(\tilde{\mathbf{B}}_1 \mid \mathbf{Y}, \boldsymbol{\Theta}_{-\mathbf{B}_1, -\mathbf{B}_2}) = \prod_{l=1}^{n_1} \mathcal{PN}(\tilde{\mathbf{b}}_{1,l}; \tilde{\mathbf{y}}_l, \mathbf{Q}_{1,l}). \quad (\text{S5})$$

where  $\mathbf{Q}_{1,l} = \mathbf{P}_l^T (\tilde{\Sigma}_l)^{-1} \mathbf{P}_l$  where  $\mathbf{P}_l = \mathbf{I} - \mathbf{H}_2 (\mathbf{H}_2^T \tilde{\Sigma}_l^{-1} \mathbf{H}_2)^{-1} \mathbf{H}_2^T \tilde{\Sigma}_l^{-1}$  for  $l = 1, \dots, d$  and  $\mathbf{Q}_{1,l} = \sigma_0^2 \mathbf{P}_0$  with  $\mathbf{P}_0 = (\mathbf{I} - \mathbf{H}_2 (\mathbf{H}_2^T \mathbf{H}_2)^{-1} \mathbf{H}_2^T)$  for  $l = d+1, \dots, n_1$ . The sample  $(\mathbf{B}_1 \mid \mathbf{Y}, \boldsymbol{\Theta}_{-\mathbf{B}_1, -\mathbf{B}_2})$  can be obtained by  $(\mathbf{H}_1^T \mathbf{H}_1)^{-1} \mathbf{H}_1^T \mathbf{A}_F \tilde{\mathbf{B}}_1^T$ , where  $\tilde{\mathbf{B}}_1$  sampled from the  $p(\tilde{\mathbf{B}}_1 \mid \mathbf{Y}, \boldsymbol{\Theta}_{-\mathbf{B}_1, -\mathbf{B}_2})$  in equation (S5).

2. After marginalizing out  $\mathbf{Z}$  and conditional on  $\mathbf{B}_1$ , the marginal posterior distribution of  $\tilde{\mathbf{B}}_2$  follows (S4) by replacing  $\tilde{\mathbf{y}}_l$  by  $\tilde{\mathbf{y}}_{l,B_1} = (\mathbf{Y} - \mathbf{H}_1 \mathbf{B}_1)^T \mathbf{a}_l$  for  $l = 1, \dots, d$ .

*Proof of Lemma S2.* Denote  $\mathbf{Y}_0 = \mathbf{Y} - \mathbf{H}_1 \mathbf{B}_1 - \mathbf{B}_2^T \mathbf{H}_2^T$ . Define  $\mathbf{G} = [\mathbf{g}_1, \mathbf{g}_2, \dots, \mathbf{g}_{n_1}] = (\mathbf{Y} - \mathbf{H}_1 \mathbf{B}_1)^T \mathbf{A}_F$ . That is,  $\mathbf{g}_l = (\mathbf{Y} - \mathbf{H}_1 \mathbf{B}_1)^T \mathbf{a}_l$ .

First we have the joint posterior distribution  $(\mathbf{B}_1, \mathbf{B}_2 \mid \mathbf{Y}, \boldsymbol{\Theta}_{-\mathbf{B}_1, -\mathbf{B}_2})$

$$\begin{aligned} &p(\mathbf{B}_1, \mathbf{B}_2 \mid \mathbf{Y}, \boldsymbol{\Theta}_{-\mathbf{B}_1, -\mathbf{B}_2}) \\ &\propto \exp \left\{ -\frac{1}{2} \sum_{l=1}^d \mathbf{a}_l^T \mathbf{Y}_0^T \tilde{\Sigma}_l^{-1} \mathbf{Y}_0 \mathbf{a}_l - \frac{1}{2\sigma_0^2} \sum_{l=d+1}^{n_1} \mathbf{a}_l^T \mathbf{Y}_0^T \mathbf{Y}_0 \mathbf{a}_l \right\} \\ &\propto \exp \left\{ -\frac{1}{2} \sum_{l=1}^d (\mathbf{g}_l - \mathbf{H}_2 \tilde{\mathbf{b}}_{2,l})^T \tilde{\Sigma}_l^{-1} (\mathbf{g}_l - \mathbf{H}_2 \tilde{\mathbf{b}}_{2,l}) - \frac{1}{2\sigma_0^2} \sum_{l=d+1}^{n_1} (\mathbf{g}_l - \mathbf{H}_2 \tilde{\mathbf{b}}_{2,l})^T (\mathbf{g}_l - \mathbf{H}_2 \tilde{\mathbf{b}}_{2,l}) \right\}, \end{aligned}$$

where  $\tilde{\mathbf{b}}_{2,l}$  is a transformation of  $\mathbf{B}_2$  defined in part 2 in Lemma S1.

After integrating out  $\tilde{\mathbf{b}}_{2,l}$  from  $p(\mathbf{B}_1, \mathbf{B}_2 \mid \mathbf{Y}, \boldsymbol{\Theta}_{-\mathbf{B}_1, -\mathbf{B}_2})$  for  $l = 1, 2, \dots, n_1$ , one has

$$\begin{aligned}
& p(\mathbf{B}_1 \mid \mathbf{Y}, \boldsymbol{\Theta}_{-\mathbf{B}_1, -\mathbf{B}_2}) \\
& \propto \exp \left\{ -\frac{\sum_{l=1}^d (\mathbf{g}_l - \mathbf{H}_2 \hat{\mathbf{b}}_{2,l})^T \tilde{\boldsymbol{\Sigma}}_l^{-1} (\mathbf{g}_l - \mathbf{H}_2 \hat{\mathbf{b}}_{2,l})}{2} - \frac{\sum_{l=d+1}^{n_1} (\mathbf{g}_l - \mathbf{H}_2 \hat{\mathbf{b}}_{2,l})^T (\mathbf{g}_l - \mathbf{H}_2 \hat{\mathbf{b}}_{2,l})}{2\sigma_0^2} \right\} \\
& \propto \exp \left\{ -\frac{\sum_{l=1}^d \mathbf{g}_l^T \mathbf{P}_l^T (\tilde{\boldsymbol{\Sigma}}_l)^{-1} \mathbf{P}_l \mathbf{g}_l}{2} - \frac{\sum_{l=d+1}^{n_1} \mathbf{g}_l^T \mathbf{P}_0 \mathbf{g}_l}{2\sigma_0^2} \right\} \\
& \propto \exp \left\{ -\frac{\sum_{l=1}^{n_1} \mathbf{g}_l^T \mathbf{Q}_{1,l} \mathbf{g}_l}{2} \right\}
\end{aligned}$$

Where

$$\hat{\mathbf{b}}_{2,l} = \begin{cases} (\mathbf{H}_2^T \tilde{\boldsymbol{\Sigma}}_l^{-1} \mathbf{H}_2)^{-1} \mathbf{H}_2^T \tilde{\boldsymbol{\Sigma}}_l^{-1} \mathbf{g}_l & l = 1, 2, \dots, d \\ (\mathbf{H}_2^T \mathbf{H}_2)^{-1} \mathbf{H}_2^T \mathbf{g}_l & l = d+1, \dots, n_1 \end{cases}$$

Denote  $\mathbf{B}_1^{aug} = [\mathbf{B}_1^T, \tilde{\mathbf{B}}_{1,(q_1+1):n_1}]^T$ , where  $\tilde{\mathbf{B}}_{1,(q_1+1):n_1}$  is the last  $n_1 - q_1$  columns of  $\tilde{\mathbf{B}}_1$ . Denote the marginal posterior distribution  $p_{trans}(\mathbf{B}_1^T \mid \mathbf{Y}, \boldsymbol{\Theta}_{-\mathbf{B}_1, -\mathbf{B}_2})$  and  $p_{trans}(\mathbf{B}_1^{aug} \mid \mathbf{Y}, \boldsymbol{\Theta}_{-\mathbf{B}_1, -\mathbf{B}_2})$  derived by the transformation of  $p(\tilde{\mathbf{B}}_1 \mid \mathbf{Y}, \boldsymbol{\Theta}_{-\mathbf{B}_1, -\mathbf{B}_2})$ . One has

$$\begin{aligned}
& p_{trans}(\mathbf{B}_1^T \mid \mathbf{Y}, \boldsymbol{\Theta}_{-\mathbf{B}_1, -\mathbf{B}_2}) \\
& \propto p(\mathbf{B}_1^{aug} \mid \mathbf{Y}, \boldsymbol{\Theta}_{-\mathbf{B}_1, -\mathbf{B}_2}) \\
& = p(\tilde{\mathbf{B}}_1 \mid \mathbf{Y}, \boldsymbol{\Theta}_{-\mathbf{B}_1, -\mathbf{B}_2}) \left| \frac{d\tilde{\mathbf{B}}_1}{d\mathbf{B}_1^{aug}} \right| \\
& \propto \exp \left\{ -\frac{\sum_{l=1}^{n_1} \mathbf{g}_l^T \mathbf{Q}_{1,l} \mathbf{g}_l}{2} \right\}
\end{aligned}$$

Because  $\mathbf{Q}_{1,l}$  is idempotent, i.e.  $\mathbf{Q}_{1,l} \mathbf{Q}_{1,l} = \mathbf{Q}_{1,l}$ , the Moore–Penrose inverse of  $\mathbf{Q}_{1,l}$  is  $\mathbf{Q}_{1,l}$  itself. Therefore for  $l = 1, \dots, d$ ,  $\tilde{\mathbf{b}}_{1,l} \mid \mathbf{Y}, \boldsymbol{\Theta}_{-\mathbf{B}_1, -\mathbf{B}_2} \sim \mathcal{M}(\tilde{\mathbf{y}}_l, \mathbf{Q}_{1,l})$ , from which the part 1 follows. Part 2 follows Lemma S1.  $\square$

We are ready to prove Theorem 2.

*Proof of Theorem 2.* By Lemma S2, the posterior mean of  $\tilde{\mathbf{B}}_1 \mid \mathbf{Y}, \boldsymbol{\Theta}_{-\mathbf{B}_1, -\mathbf{B}_2}$  is  $\mathbf{Y}^T \mathbf{A}_F$ , where  $\mathbf{A}_F := [\mathbf{A}_s, \mathbf{A}_c]$ . We denote the centered  $\tilde{\mathbf{B}}_1$  by  $\tilde{\mathbf{B}}_{1,0} = [\tilde{\mathbf{B}}_{1,Q}, \tilde{\mathbf{B}}_{1,0,c}] = \tilde{\mathbf{B}}_1 - \mathbf{Y}^T \mathbf{A}_F$ , where  $\tilde{\mathbf{B}}_{1,Q}$  is the first  $d$  columns of  $\tilde{\mathbf{B}}_{1,0}$  and  $\tilde{\mathbf{B}}_{1,0,c}$  is the next  $(n_1 - d)$  columns of  $\tilde{\mathbf{B}}_{1,0}$ . Then the posterior mean of  $\mathbf{B}_1 \mid \mathbf{Y}, \boldsymbol{\Theta}_{-\mathbf{B}_1, -\mathbf{B}_2}$  can be calculated below

$$\begin{aligned}
\hat{\mathbf{B}}_1 &= \mathbb{E}(\mathbf{B}_1 \mid \mathbf{Y}, \boldsymbol{\Theta}_{-\mathbf{B}_1, -\mathbf{B}_2}) = \mathbb{E} \left( (\mathbf{H}_1^T \mathbf{H}_1)^{-1} \mathbf{H}_1^T \mathbf{A}_F \tilde{\mathbf{B}}_1^T \mid \mathbf{Y}, \boldsymbol{\Theta}_{-\mathbf{B}_1, -\mathbf{B}_2} \right) \\
&= (\mathbf{H}_1^T \mathbf{H}_1)^{-1} \mathbf{H}_1^T \mathbf{A}_F \mathbf{A}_F^T \mathbf{Y} = (\mathbf{H}_1^T \mathbf{H}_1)^{-1} \mathbf{H}_1^T \mathbf{Y}
\end{aligned}$$

Note  $\mathbf{B}_1 = (\mathbf{H}_1^T \mathbf{H}_1)^{-1} \mathbf{H}_1^T \mathbf{A}_F \tilde{\mathbf{B}}_1^T$ , one has

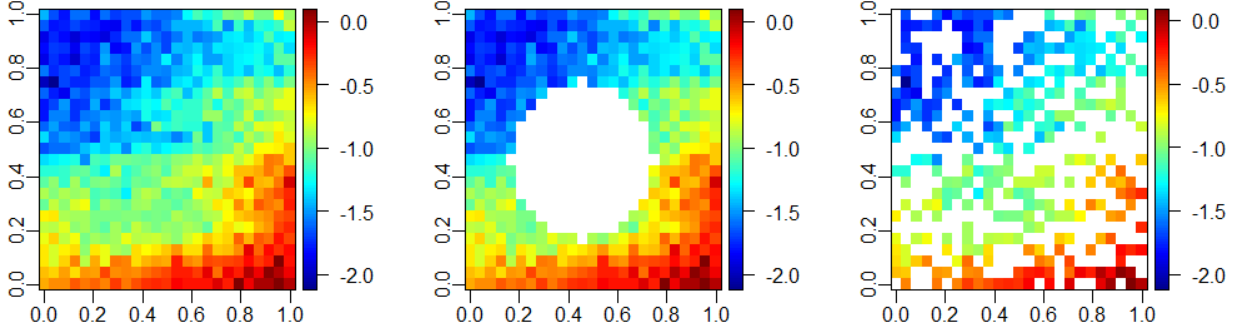


Figure S1: The simulated data with full observations, disk missing pattern and missing-at-random pattern with 50% of the missing values are graphed in the left, middle and right panels, respectively.

$$\mathbf{B}_1 - \hat{\mathbf{B}}_1 = (\mathbf{H}_1^T \mathbf{H}_1)^{-1} \mathbf{H}_1^T \mathbf{A}_F (\tilde{\mathbf{B}}_{1,0})^T = (\mathbf{H}_1^T \mathbf{H}_1)^{-1} \mathbf{H}_1^T (\mathbf{A}_s (\tilde{\mathbf{B}}_{1,Q})^T + \mathbf{A}_c (\tilde{\mathbf{B}}_{1,0,c})^T)$$

where by Lemma S2,  $\tilde{\mathbf{B}}_{1,Q}$  is an  $n_2 \times d$  matrix with the  $l$ th column independently sampled from  $\mathcal{N}(\mathbf{0}, \mathbf{Q}_{1,l})$  for  $l = 1, \dots, d$ . For the distribution of  $\mathbf{A}_c \tilde{\mathbf{B}}_{1,0,c}^T$ , using part 1 of Lemma S2, we have

$$\begin{aligned} & p(\mathbf{A}_c \tilde{\mathbf{B}}_{1,0,c}^T | \mathbf{Y}, \boldsymbol{\Theta}_{-B_1, -B_2}) \\ & \propto \exp \left\{ \frac{1}{2\sigma_0^2} \text{tr} \left( \mathbf{A}_c \mathbf{A}_c^T \tilde{\mathbf{B}}_{1,0,c} \mathbf{P}_0 (\tilde{\mathbf{B}}_{1,0,c})^T \right) \right\} \\ & \propto \exp \left\{ -\frac{1}{2\sigma_0^2} \text{tr} \left( (\mathbf{I} - \mathbf{A}_s \mathbf{A}_s^T) \tilde{\mathbf{B}}_{1,0,c} \mathbf{P}_0 (\tilde{\mathbf{B}}_{1,0,c})^T \right) \right\}. \end{aligned}$$

Thus we can sample marginal posterior distribution of  $\mathbf{A}_c \tilde{\mathbf{B}}_{1,0,c}^T$  by  $\sigma_0(\mathbf{I} - \mathbf{A}_s \mathbf{A}_s^T) \mathbf{Z}_{0,1} \mathbf{P}_0$ , where  $\mathbf{Z}_{0,1}$  is an  $n_1 \times n_2$  matrix with each entry independently sampled from standard normal distribution. The results soon follow.  $\square$

## S2 Additional results of simulated studies in Section 5

We provide additional results for the simulated studies in Example 3 in Figure S1 and Figure S2. We graph the simulated data set with full observations, disk missing pattern and missing-at-random pattern with 50% of the missing values in Figure S1. The posterior samples of the logarithm of the inverse range parameter of factor loading matrix, the nugget parameter and the inverse range parameter of the factors are graphed from the upper to lower panels in Figure S2, respectively. The posterior samples of parameters in the exact GP model and GOLF processes are similar to each other.

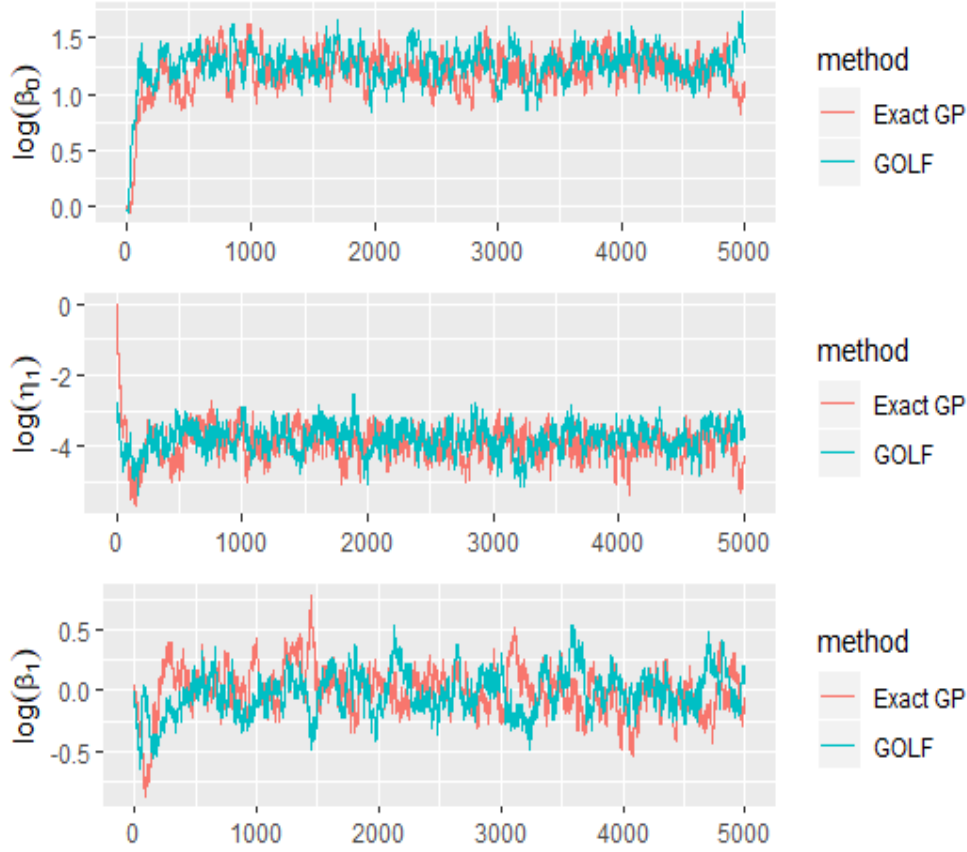


Figure S2: Trace plots of the posterior samples of the parameters in the exact GP model and the GOLF processes for the simulated data in figure S1.

### S3 Additional results for real applications in Section 6.1

In this section, we include additional results for GOLF processes predicting the missing values of the temperature data set discussed in Heaton et al. (2019). We show the details of 5 different configurations of GOLF processes, where the result reported in the main body of the article is the configuration 1. For all the configurations, the proportion of the burn-in samples is 20%. We use the normal distribution centered on the previous values as the proposal distribution of the logarithm of the inverse range parameters and logarithm of the nugget parameters. For the logarithm of the inverse range parameters of the factor loading matrix, the standard deviation of the proposal distribution is  $40/n_1$ . For the logarithm of the inverse range parameters and the nugget parameters of the factor processes, the standard deviation of the posterior distribution is set to be  $40/n_2$ .

The details of 5 configurations are given in Table S1. The predictive RMSE,  $P_{CI}(95\%)$  and  $L_{CI}(95\%)$  of the 5 configurations are given in Table S2. The predictive RMSE is similar for all 5 configurations. Increasing the posterior sample size seems to slightly increase the proportion of the samples contained in the 95% predictive interval.

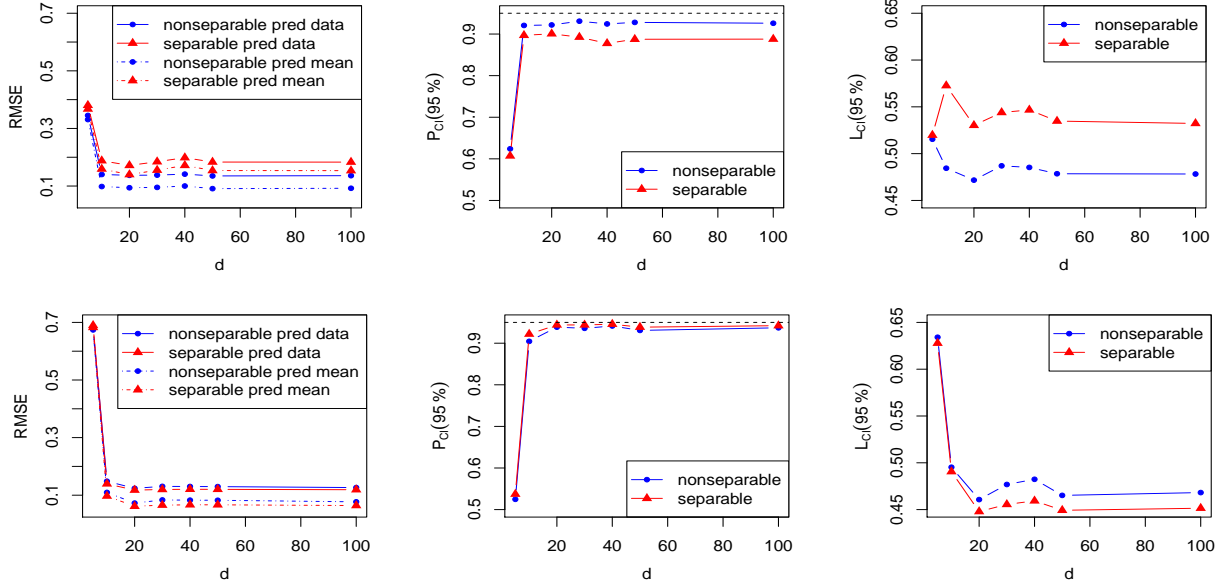


Figure S3: The predictive performance of GOLF process with  $d = 5, 10, 20, 30, 40, 50$  and 100 factors for Example 4, when the true number of factor is  $d_{real} = 100$  in generating the data. The nonseparable kernel with distinct kernel parameters is assumed to generate the data in the first row of panels, and separable kernel with the same kernel parameter of each factor process is used for simulation in the second row of panels. The blue curves and red curves denote the performance by the GOLF processes with the different kernel parameters and the same kernel parameter, respectively. In the left panels, the solid curves denote the RMSE for predicting the (noisy) observations, and the dashed curve denote the RMSE for predicting the mean of the observations. The proportions of observations covered in the 95% predictive interval and the average length of the predictive interval are graphed in the middle and right panels, respectively.

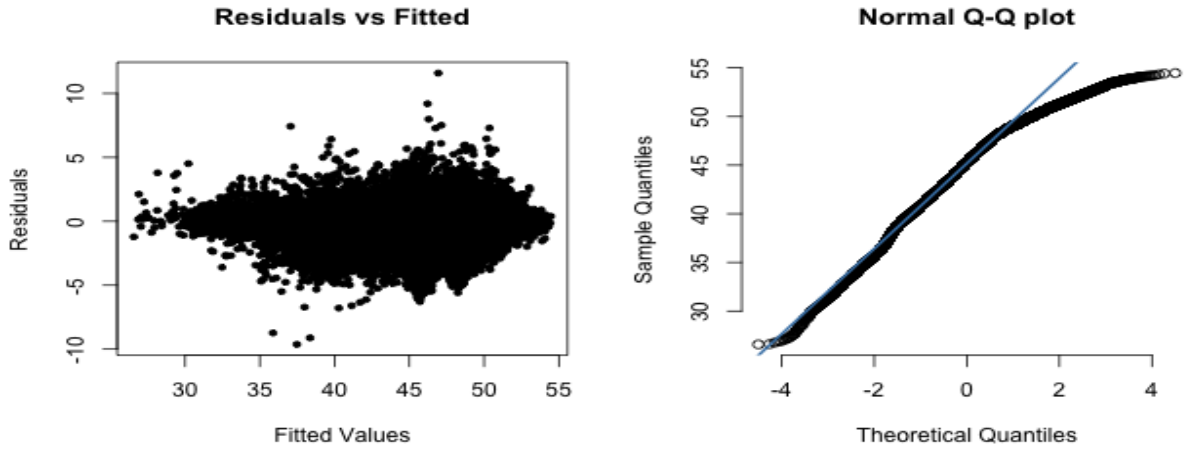


Figure S4: Diagnostic plots of the GOLF processes for the data set in Heaton et al. (2019).

	sample size	system	initial $Y_{v,i}^*$	initial $\log(\beta_0)$	initial $\log(\beta_l)$
Conf. 1	6000	Mac	mean at each latitude	3	0
Conf. 2	6000	Win	mean at each latitude	3	0
Conf. 3	40000	Mac	mean at each latitude	3	0
Conf. 4	40000	Mac	overall mean + noise	3	0
Conf. 5	40000	Mac	mean at each latitude	Unif[-1,1]	Unif[-1,1]

Table S1: Detailed settings of 5 different configurations of GOLF processes for the data set in Heaton et al. (2019). The number of samples and the computing system are shown in the second column and third column, respectively. The choice of the initial values of the missing data is given in the fourth column, using either the mean of the observations at each latitude or overall mean of the observations with a small random Gaussian noise (with standard deviation being 0.1 times of the standard deviation of the observations). The initial values of the logarithm of the inverse range parameters are either chosen to be a fixed value or randomly sampled from the uniform distribution, shown in column 5-6.

Methods	RMSE	$P_{CI}(95\%)$	$L_{CI}(95\%)$
Configuration 1	1.46	0.92	4.95
Configuration 2	1.50	0.91	4.92
Configuration 3	1.44	0.94	7.70
Configuration 4	1.48	0.94	7.75
Configuration 5	1.51	0.93	5.16

Table S2: Predictive performance of 5 different implementations for the data set in Heaton et al. (2019).

The fitted values from the GOLF processes in configuration 1 against the residuals and the normal Q-Q plot are graphed in left panel and the right panel in Figure S4, respectively. The Q-Q plot indicates the fitted values are slightly left-skewed and slightly under-dispersed.